Ms H-00185-2018-R2

Na/Ca exchanger overexpression in smooth muscle augments cytosolic Ca^{2+} in femoral arteries of living mice

Jin Zhang[1,*], Youhua Wang[1,2,*,†], Ling Chen[1,3], W. Gil Wier[1,4,§] and Mordecai P. Blaustein[1,3]

Departments of [1]Physiology and [3]Medicine, University of Maryland School of Medicine, Baltimore, MD, USA; [2]Department of Physical Education, Shaanxi Normal University, Xi'an, Shaanxi, China; [4]Department of Physiology, University of Maryland School of Medicine, Baltimore, MD, USA

Running Title: NCX overexpression and arterial $[Ca^{2+}]_{CYT}$

***These authors contributed equally to this work**

†**Present address:** Department of Physical Education, Shaanxi Normal University, Xi'an, Shaanxi, China

§**Present address:** Department of Physiology, University of Maryland School of Medicine, Baltimore, MD, USA

Address correspondence to:
Mordecai P. Blaustein, M.D.
Department of Physiology
University of Maryland School of Medicine
655 W. Baltimore St.
Baltimore, MD 21201
Ph: 410-706-3345
Fax: 410-706-8341
Email: mblaustein@som.umaryland.edu

Key words: Arterial tone, SEA0400, sodium nitroprusside, vasodilation,

Abbreviations: ACh, acetylcholine; ACTH, adrenocorticotropic hormone; Ang II, angiotensin II; ANOVA, analysis of variance; ASMCs, arterial smooth muscle cells; BP, arterial blood pressure; CFP, cyan fluorescent protein; CO, cardiac output; Ctrl, control; DMSO, dimethylsulfoxide; eGFP, enhanced green fluorescent protein; exMLCK, exogenous myosin light chain kinase; FRET, fluorescent resonance energy transfer; iv, intravenous; KO, knockout; NCX, Na^+/Ca^{2+} exchange; NO, nitric oxide; PD, passive diameter; PE, phenylephrine; SERCA, sarcoplasmic reticulum Ca^{2+} pump; SM, smooth muscle; SNA, sympathetic nerve activity; SNP, Na^+ nitroprusside; SR, sarcoplasmic reticulum; TG, transgenic; TPR, total peripheral resistance; TRP, transient receptor potential; YFP, yellow fluorescent protein

New and Noteworthy:

Smooth muscle Na/Ca exchanger-1 transgene overexpression (TG mice) increases femoral artery basal cytosolic Ca^{2+} ($[Ca^{2+}]_{CYT}$) and tone in vivo and raises blood pressure (BP). Arterial constriction to phenylephrine and angiotensin II are normal, but superimposed on the augmented basal $[Ca^{2+}]_{CYT}$ and tone (constriction) in TG mouse arteries. Similar effects in resistance arteries would explain the elevated BP. Acetylcholine-induced vasodilation is unimpaired, implying a normal endothelium, but TG arteries are hypersensitive to sodium nitroprusside (NO donor).

ABSTRACT

The plasma membrane Na/Ca exchanger-1 (NCX1) helps regulate the cytosolic Ca^{2+} concentration ($[Ca^{2+}]_{CYT}$) in arterial myocytes. NCX1 mediates both Ca^{2+} entry and exit, and tends to promote net Ca^{2+} entry in partially-constricted arteries. Mean BP (telemetry) is elevated by ≈10 mm Hg in transgenic (TG) mice that overexpress NCX1 specifically in smooth muscle. We tested the hypothesis that NCX1 overexpression mediates Ca^{2+} gain and elevated $[Ca^{2+}]_{CYT}$ in exposed femoral arteries that also express the Ca^{2+} biosensor, exMLCK. $[Ca^{2+}]_{CYT}$ and the NCX1-dependent (SEA0400-sensitive) component, ≈15% of total basal constriction in controls, were increased in TG arteries, but constrictions to phenylephrine (PE) and angiotensin II (Ang II) were comparable in TGs and controls. Normalized PE dose-response curve and constriction to 30 and 300 ng/kg iv Ang II were virtually identical in control and TG arteries. Ang II-evoked constrictions, superimposed on elevated basal tone, accounts for the larger BP responses to Ang II in the TGs. TG and control mouse arteries fit the same pCa-constriction relationship over a wide range of pCa (≈125-500 nM). Vasodilation to acetylcholine (ACh), normalized to passive diameter (PD), also was comparable in TGs and controls, implying normal endothelial function. TG artery Na^+ nitroprusside (SNP, an NO donor)-induced dilations were, however, shifted to lower SNP concentrations, indicating that TG myocyte vasodilator mechanisms were augmented. Maximum arterial dilation was comparable in TG and control mice although PD was ≈6-7% smaller in TGs. The changes in TG arteries were apparently largely functional rather than structural despite the congenital hypertension.

INTRODUCTION

Calcium homeostasis plays a fundamental role in vasoconstriction and hemodynamics because Ca^{2+} ions trigger contraction in vascular smooth muscle (47). The plasma membrane (PM) Na/Ca exchanger (NCX) is unique among the many ion channels and transporters that normally regulate the cytosolic Ca^{2+} concentration ($[Ca^{2+}]_{CYT}$) and signaling in arterial smooth muscle cells (ASMCs). NCX can transport Ca^{2+} either into or out of ASMCs, depending upon the Na^+ and Ca^{2+} concentration gradients and the membrane potential (V_M). The net NCX-mediated Ca^{2+} flux direction, inward or outward, is determined by the net driving force on the exchanger, $V_M - E_{Na/Ca}$, where $E_{Na/Ca} = 3E_{Na} - 2E_{Ca}$, and E_{Na} and E_{Ca} are, respectively, the Na^+ and Ca^{2+} equilibrium potentials (9). In cardiomyocytes during diastole, and in quiescent neurons, V_M is on the order of -70 mV, and is more negative than $E_{Na/Ca}$; thus, NCX mediates Ca^{2+} efflux, primarily, in these cells. Most ASMCs are tonically contracted in vivo in order to maintain arterial tone, and V_M is generally about -30 to -45 mV (29, 32) and is more positive than the calculated $E_{Na/Ca}$[1]. NCX should therefore mediate Ca^{2+} influx, primarily, in ASMCs (23, 44, 61, 62). In this case, overexpression of NCX would be expected to enhance Ca^{2+} influx, elevate $[Ca^{2+}]_{CYT}$, augment Ca^{2+} signaling and arterial tone, and increase blood pressure (BP). In fact, transgenic (TG) mice that overexpress NCX type-1 specifically in smooth muscle (SM-NCX1-TG mice) have elevated BP and enhanced salt-sensitivity (23).

---

[1]The $E_{Na/Ca}$ should be determined from the local cytosolic Na^+ concentration ($[Na^+]_{CYT}$) in the vicinity of NCX, assuming that the extracellular Na^+ and Ca^{2+} concentrations and $[Ca^{2+}]_{CYT}$ are known. In ASMCs, the calculation is based on an estimated global $[Na^+]_{CYT}$ (2, 26). In tonically constricted arteries, however, the local $[Na^+]_{CYT}$ (and $[Ca^{2+}]_{CYT}$) in the vicinity of NCX might be elevated due to Na^+ entry through various transient receptor potential (TRP protein) channels which admit Na^+ and Ca^{2+} (16). Furthermore, V_M, $[Na^+]_{CYT}$ and $[Ca^{2+}]_{CYT}$, and thus, $E_{Na/Ca}$ and $V_M - E_{Na/Ca}$, all vary dynamically.

The discovery of NCX in arterial smooth muscle fostered the view that the cooperative action of PM Na^+ pumps and NCX contributes to the regulation of ASMC $[Ca^{2+}]_{CYT}$ and BP (6, 46). Indeed, NCX1 and ouabain-sensitive $\alpha 2$ Na^+ pumps, as well as certain receptor- and store-operated (TRP) channels that are permeable to Na^+ and Ca^{2+}, co-localize in PM microdomains at ASMC PM-sarcoplasmic reticulum (SR) junctions ("PLasmERosomes" (3, 8, 27, 65)). Together these transporters all help regulate local $[Na^+]_{CYT}$ and $[Ca^{2+}]_{CYT}$, and SR Ca^{2+} stores in human and rodent ASMCs (34, 39, 54).

Expression of NCX1, and of the SR Ca^{2+} pump (SERCA) and several Ca^{2+}-selective channels is increased in ASMCs in many animal models of hypertension (10, 42, 65). This Ca^{2+} transporter 'protein remodeling' appears to be due to a direct action of ouabain on $\alpha 2$ Na^+ pumps because incubation of primary cultured rodent or human ASMCs with nanomolar ouabain also up-regulates these proteins (34, 43). Moreover, mice with mutant, ouabain-resistant $\alpha 2$ Na^+ pumps do not develop ouabain-induced or ACTH-induced hypertension, and the NCX blocker, KBR7943, prevents the development of ACTH-induced hypertension (14, 15, 36). These studies indicate that the $\alpha 2$ Na^+ pump ouabain binding site and NCX1 are intimately involved in the control of Ca^{2+} homeostasis and BP, and contribute to the generation of many forms of hypertension.

Given this key role of NCX1 in arteries, the present report describes experiments designed to test the hypothesis that arterial NCX1-mediated Ca^{2+} entry is enhanced in SM-NCX1-TG mice, thereby increasing basal $[Ca^{2+}]_{CYT}$ and augmenting Ca^{2+} signaling and constriction in vivo. The studies were performed on exposed femoral arteries of live, anesthetized mice because: *i*) Simultaneous $[Ca^{2+}]_{CYT}$ and diameter measurements have been validated in this preparation (60); *ii*) The effects of local and systemic application of various pharmacological agents can be assessed in vivo - e.g., femoral artery $[Ca^{2+}]_{CYT}$ is increased and diameter is decreased in mice with angiotensin (Ang) II-induced hypertension (58); and, *iii*). The effects of genetic engineering (e.g., arterial NCX1 overexpression) on arterial $[Ca^{2+}]_{CYT}$ and diameter also can be measured directly. Since NCX1-TG mice are modestly hypertensive (23) and

endothelium-dependent vasodilation is often attenuated in hypertension (55), acetylcholine (ACh)-induced vasodilation was also examined.

BP is determined largely by the 'tone' (constriction as a percent of passive diameter) in small 'resistance arteries', with only a small contribution from constriction of large muscular arteries such as the femoral artery (4, 17). Nevertheless, most of the same vasoconstrictor and vasodilator receptors, and Ca^{2+} transporter proteins, including NCX1, are expressed in resistance as well as muscular arteries (39, 41, 57, 61, 62), even though quantitative differences in Ca^{2+} handling surely contribute to functional dissimilarities. We reasoned that the effects of NCX1 upregulation and increased Ca^{2+} delivery on femoral artery Ca^{2+} signaling and diameter in vivo might also provide clues to the effects of NCX1 upregulation in resistance arteries. Indeed, the enhanced myogenic tone in isolated small resistance arteries of TG mice (unpublished) seems consistent with the enhanced sympathetic drive-dependent tone in the femoral arteries of TG mice (this report). Thus, despite the likely compensatory action of other transporters which may be differently regulated in different vascular beds, enhanced Ca^{2+} delivery mediated by upregulated NCX1 and its effects on arterial constriction appeared to dominate.

Notwithstanding the elevated basal arterial $[Ca^{2+}]_{CYT}$ and BP in TGs, vasoconstrictor-evoked Ca^{2+} signals and ACh-induced vasodilation were comparable in control and TG mouse femoral arteries. These results, which are contrary to expectation, may provide novel insight into some of the peripheral mechanisms that contribute to the pathogenesis of hypertension.

MATERIALS AND METHODS

Experimental mice and ethical approval

All husbandry and experimental procedures involving mice complied with the standards stated in the National Institutes of Health Guide for the Care and Use of Laboratory Animals and were approved by the University of Maryland Baltimore (UMB) Institutional Animal Care and Use Committee (IACUC). The mice were housed in the UMB Veterinary Resources facility and were fed standard laboratory chow.

The SM-NCX1-TG mice (designated $N1.3^{Tg/Tg}$-10) were originally generated by Prof. Takahiro Iwamoto (Fukuoka University, Fukuoka, Japan) (23). The transgene was randomly inserted into the genome so that mice may have several copies of the gene and greatly over-express the protein [Fig. 1 and Supplementary Fig. 3 in (23)] but the copy number in each mouse was not determined. The mice were generously provided to us by Prof. Iwamoto, and the mouse line was re-derived on a C57Bl/6 background. It was then crossed with a line that expresses a modified exogenous myosin light chain kinase transgene (exMLCK) in smooth muscles (60); exMLCK is a green fluorescent protein (eGFP)-based cyan/yellow fluorescent protein (CFP/YFP) FRET Ca^{2+} biosensor (18). The offspring exMLCK/SM-NCX1-TG mice (on a C57Bl/6 background), were then inbred to generate mice homozygous for both transgenes. For convenience the inbred mice will be designated as 'NCX1-TG' or 'TG' mice. Mice that expressed exMLCK, but not the NCX1 transgene, were used as controls ("Ctrl"). The presence of the exMLCK gene has no detectable effect on the contractile and hemodynamic properties of the arteries (60).

In a few experiments (see Results), mice in which NCX1 was conditionally knocked out in smooth muscle (SM-NCX1-KO mice, abbreviated as "KO") (57) were tested for comparison with the control and TG mice.

The following are the primer set sequences employed for genotyping the mice with the two transgenes: 1. exMLCK forward, 5'-GCACGACTTCTTCAAGTCCGCCATGCC-3'; 2. exMLCK

reverse, 5'- GCGGATCTTGAAGTTCACCTTGATGCC-3'; 3. NCX1 forward, 5'-AGGTGAAGGTATTGCGAACATCTGGA-3'; and 4. NCX1 reverse, 5'-GGCTCCAATGAAAGCTGTCAGTAT-3'.

Blood pressure measurements

Telelemtry: Telemetric BP transmitters (DSI TA11PA-C10, Data Sciences International, Minneapolis, MN, USA) were surgically implanted in 15-18 week old mice in the UMB IACUC-approved Physiology Phenotyping Core. The transmitter catheter was inserted into the right common carotid artery, and the tip was threaded into the ascending aorta. Details are published (62). Following 7-10 days of recovery from surgery, 24 hr BPs were recorded with DSI receivers and software. After stable baseline BPs were recorded, under isoflurane anesthesia, Alzet osmotic minipumps (Durect Corp., Cupertino, CA, USA) were implanted in the right abdominal wall for subcutaneous (sc) infusion of angiotensin II (Ang II) or vehicle. The 24 hr BP data collection was performed "double-blind": the individual measuring the BP did not know the genotype. Animal code numbers were matched with genotype and BP after the data had been collected.

Acute aortic BP measurements. Mice, ~15-18 weeks old, were anaesthetized with 2-3% isoflurane supplemented with 100% O_2; core temperature was maintained at 37.5-38^{o}C. An anterior midline incision was made in the neck, and the right carotid artery and jugular vein were isolated and the trunk of the carotid was ligated with a suture. A 1.1 French Mikro-tip pressure catheter (Millar Instruments, Houston, TX, USA) was inserted into the artery proximal to the ligature and threaded forward to the ascending aorta. The jugular vein was then ligated and a PE-10 catheter (Braintree Scientific, Braintree, MA, USA) for intravenous (iv) infusions was inserted caudally and threaded down to the superior vena cava. The incision was then closed with 5-mm EZ clips (Braintree). Arterial BP was recorded under 1.5% isoflurane anesthesia (25) at a sampling rate of 1 kHz using a PowerLab data acquisition system (AD Instruments, Colorado Springs, CO, USA). Data were later calculated off-line (BioPac System,

Santa Barbara, CA, USA). After the experiment, the animal was deeply anesthetized with isoflurane and euthanized by cervical dislocation. Further details are given in (60).

Femoral artery in vivo imaging

The in vivo imaging methods and validation have been described in detail (58, 60). In brief, under microscope observation, a femoral artery of an isoflurane-anesthetized mouse was exposed through a cutaneous incision in the mid-thigh. The connective tissue was lightly dissected over a ~2 mm long region of the distal part of the femoral artery, taking care to avoid severing nerves. The mouse was then moved to the stage of the fluorescence microscope, and superfusion of the exposed artery and surrounding muscle was initiated. The arrangement of the inlet and outlet for the superfusion fluid was made to achieve a laminar flow over the artery of ~9 ml/min.

The use of a volatile anesthetic (isoflurane) was desirable to maintain the animal in an optimal physiological state. Such agents have, however, been reported to influence sympathetic nerve activity (49), alter the activity of the renin/angiotensin system (53), and activate K^+ channels (30). Nevertheless, femoral arteries under the conditions of these experiments maintained a high degree of vasoconstriction, as evidenced by the large increase in diameter after total autonomic ganglion blockade (see Results).

Fluorescence and diameter recording in femoral arteries

A xenon arc lamp (Lambda LS, Sutter Instrument, Novato, CA, USA) provided intensity-adjusted, gated fluorescent illumination at 436 ± 10 nm (excites CFP) that was controlled by a programmable shutter (Smart Shutter, Sutter Instrument). A long working distance, high numerical aperture Olympus MVX10 MacroView fluorescence microscope (Olympus America, Center Valley, PA, USA) and a sensitive charge-coupled device ORCA ER camera (Hammamatsu, Bridgewater, NJ, USA) fitted with a DualView image splitter (Photometrics, Tucson, AZ, USA) were employed. This provided "CFP" and "YFP" images (470 and 535 nm, respectively). The camera was controlled and images were acquired (1 frame/s) using HCImage (Hamamatsu). Image processing was performed with custom software written using IDL 6.4 (IIT Visual Information Solutions, Boulder, CO, USA). Elevation of

$[Ca^{2+}]_{CYT}$ promotes the binding of Ca^{2+} to calmodulin and exMLCK (a calmodulin-based biosensor (22)). In the latter case, the CFP and YFP moieties then move apart, thereby reducing Förster Resonance Energy Transfer (FRET) from CFP to YFP and, thus, increasing the CFP/YFP (FRET) ratio. The FRET ratio was calibrated to determine $[Ca^{2+}]_{CYT}$; (60) provides details.

Arterial 'tone' is the difference between the passive diameter in Ca^{2+}-free solution (PD) and the observed diameter under basal or other conditions tested (D_{Obs}) as a percent of PD:

$$\text{Tone} = \frac{\text{PD} - \text{D Obs}}{\text{PD}} \text{ x } 100.$$

Changes in D_{Obs} (ΔD_{Obs}) due to agent applications are presented as a percent of PD [(ΔD_{Obs}/PD) x 100]. Vasodilation is graphed as upward bars or curves, vasoconstriction is graphed as downward bars or curves. Actual diameters are also graphed.

Immunoblotting

Published methods were employed for immunoblotting of mouse aorta membrane proteins (34, 61, 62). NCX1 expression was identified by chemiluminescence with R3F1 anti-NCX1 monoclonal antibodies (R3F1, generously provided by Prof. Kenneth D. Philipson, UCLA, Los Angeles, CA, USA). β-Actin was used as a loading control and was identified with clone AC-74 anti-β-actin monoclonal antibodies (Sigma-Aldrich, St. Louis, MO, USA).

Reagents and solutions

Artery superfusion solution (in mM): 112 NaCl, 25.7 $NaHCO_3$, 4.9 KCl, 2.5 $CaCl_2$, 1.2 $MgSO_4$, 1.2 KH_2PO4, 11.5 glucose, and 10 HEPES (pH 7.4, equilibrated with gas of 5% O_2, 5% CO_2 and 90% N_2 at 37°C). Ca^{2+}-free solution was made by omitting Ca^{2+} and adding 0.5 mM EGTA.

Reagents and sources were as follows: ACh, angiotensin II (Ang II), hexamethonium chloride, sodium nitroprusside (SNP), ouabain, phenylephrine (PE), and prazosin HCl (Sigma-Aldrich); losartan (Merck & Co., Kenilworth, NJ, USA); SEA0400 (2-[4-[(2,5-difluorophenyl) methoxy]phenoxy]-5-

ethoxyaniline) was a gift from Prof. Iwamoto. All reagents were reagent grade or the highest grade available. SEA0400 was dissolved in DMSO; other agents were dissolved in double-distilled, deionized water as stock solutions. The final bath concentration of DMSO did not exceed 0.01% (v/v) and did not affect vascular function.

Statistics

Data in the figures are shown as means ± S.E. The Shapiro-Wilk and Levene tests were performed for, respectively, data normality and homogeneity; all data use for ANOVA passed both tests. Paired or unpaired t-tests, or 2-way ANOVA with post-hoc correction using the Bonferroni approach, or linear regression (SigmaPlot 11.0; Systat Software, San Jose, CA) were used to test for significant differences ($P<0.05$), as stated in the figure legends. SigmaPlot was used for post-hoc calculation of statistical power.

RESULTS

NCX1 expression detected by immunoblotting and function

Relative NCX1 expression was determined by immunoblotting. NCX1 expression was markedly up-regulated in aortas from NCX1-TG heterozygous mice, and even more so in homozygous TG mice (Fig. 1) because each mouse may have several copies of the transgene. These results resemble those obtained with the original TG line (Supplementary Fig. 3a in (23)). Homozygous overexpressors were used for all experiments described below.

Functional evidence of NCX1 overexpression was obtained in femoral arteries of anesthetized mice in vivo. First, arterial diameter and $[Ca^{2+}]_{CYT}$ were measured in control and TG mouse arteries. Under basal conditions, the average diameter of TG arteries was about 20% narrower than that of controls, whereas the passive diameters (PDs) of TG arteries (i.e., in Ca^{2+}-free solution) were only about 5% narrower than the PDs of controls (Fig. 2A and legend). Basal "tone" was, therefore, significantly greater in the TG femoral arteries (Fig. 2B). This increased tone was associated with, and is likely due to, the significantly elevated basal $[Ca^{2+}]_{CYT}$ in the TG arteries (Fig. 2C). The modestly smaller PD of the TG arteries in age-matched mice raises the possibility that the congenital increase in arterial tone and BP ((23) and this report) may have induced some structural changes in the TG arteries.

Second, to test for NCX1 function directly, the effects of the NCX1 inhibitor, SEA0400, on $[Ca^{2+}]_{CYT}$ and femoral artery diameter were determined. Superfusion with 0.3 μM SEA0400 reduced $[Ca^{2+}]_{CYT}$ by ~50 nM in control arteries, but by ~85 nM in the TG arteries (Fig. 3A,B). This was associated with significantly greater decrease in tone in the TG than the control arteries (Fig. 3C,D), as expected if the arterial constriction and tone depend, in part, upon NCX1-mediated, SEA0400-sensitive Ca^{2+} entry. The SEA0400-induced 30% decline in basal tone in the TG mouse arteries was statistically significant, but the 10% decline in the control arteries was not even though all 6 arteries dilated by a small amount.

Further, when the arteries were constricted by prolonged (15 min) exposure to 10 μM ouabain, which should elevate $[Na^+]_{CYT}$ and promote Ca^{2+} entry via NCX1 (Fig. 4A), the TG arteries constricted more than did the controls (Fig. 4B). SEA0400 then reduced the constriction in TG arteries to a significantly greater extent than in the controls (Fig. 4B). The elevated basal $[Ca^{2+}]_{CYT}$ in arteries from TG mice and the difference in SEA0400-triggered decrease in tone between control and TG mice fit the view that ASMC NCX1 mediates Ca^{2+} entry, primarily, in these arteries with tone. The data in Figs 2-4 are all consistent with the overexpression of NCX1 protein in TG mouse arteries (Fig. 1).

Basal BP and the BP responses to chronic and acute Ang II infusion are augmented in TG mice

The BP data in Fig. 5A supports previous reports (23, 57, 62) that SM-NCX1 knockout (KO) reduces basal BP and SM-NCX1 overexpression elevates BP relative to BP in control mice. Furthermore, the BP increase induced by chronic low dose sc Ang II infusion (400 ng/kg/min for 3 weeks) was much greater in the TG mice, and less in KO mice, than in controls. Also, acute iv infusion of 30 and 300 ng/kg Ang II induced a significantly larger increment in BP in TG than in control anesthetized mice (Fig. 5B). This raises the possibility that arteries from TG mice may be more sensitive to Ang II than arteries from control mice and that the Ang II dose-response curve may therefore be shifted to the left.

Femoral artery tone is largely dependent upon sympathetic drive

Femoral arteries in vivo constricted to superfused PE, the α1 adrenoceptor agonist, in a dose-dependent manner (Fig. 6). Basal $[Ca^{2+}]_{CYT}$ was elevated in TG arteries (Figs. 2C and 3A) and they were modestly, but significantly more constricted than control arteries at baseline (Figs. 2A, 6A; and see Figs 7-11). Furthermore, the TG artery diameter-PE dose-response curve was shifted downward relative to the curve for control arteries (Fig. 6A). When the data were normalized to PD and expressed as PE-induced vasoconstriction and $\Delta[Ca^{2+}]_{CYT}$ vs PE concentration curves, however, the control and TG artery curves were almost superimposable (Figs. 6B, C). Thus, the sensitivity of the TG arteries to PE appeared comparable to that of the control arteries.

Superfusion of femoral arteries with 300 nM prazosin, an α1 adrenoceptor antagonist, reduced arterial $[Ca^{2+}]_{CYT}$ to ≈80-85 nM in both TG and control anesthetized mice, and dilated the arteries and decreased basal tone by about 55% in controls and 70% in TGs (Fig. 7A-C). The decrease in tone in WT arteries was only modestly greater than the 46% decline observed with 100 nM prazosin (59). Of note, prazosin reduced tone to about the same level (≈12-14 % of PD) in TG and control arteries. This implies that the TG-induced increase in tone apparently depended upon both the NCX1-mediated increase in $[Ca^{2+}]_{CYT}$ (Fig. 3) and the sympathetic nerve activity (SNA).

Blockade of the autonomic ganglia by iv bolus infusion of 3 mg/kg hexamethonium reduced $[Ca^{2+}]_{CYT}$ to barely measurable levels, and dilated the arteries almost to PD, thereby nearly abolishing tone in both TG and control mice (Fig. 8A-D). These effects of prazosin and hexamethonium indicate that the higher $[Ca^{2+}]_{CYT}$ and greater tone in the TG mouse femoral arteries both depend largely upon SNA. The hexamethonium data signify that essentially all of the basal tone in TG arteries, as in controls (see (59)), was due to sympathetic drive. Also, the mean PDs of Ctrl and TG arteries were nearly identical (Fig. 2 legend), even though the TG arteries had significantly more basal tone (Figs. 2B, 3C, and 7A).

In both control and TG femoral arteries, 100 nM Ang II superfusion elevated $[Ca^{2+}]_{CYT}$, induced vasoconstriction, and increased tone, and the magnitudes of these changes were comparable in the TG and control arteries (Fig. 9A-C). Further, 100 nM losartan, the Ang II type-1 receptor (AT_1R) antagonist, abolished all of these Ang II-induced changes (Fig. 9A-C). Both the PE and Ang II data (Figs. 6 and 9) indicate that arterial contractility is comparable in control and TG mice. In comparison to the sympatholytic agents (Figs. 7 and 8), however, losartan had negligible effect on $[Ca^{2+}]_{CYT}$, basal diameter and tone in either control or TG arteries (Fig. 10A-C). Thus, Ang II activation apparently contributes very little to basal tone, in contrast to the dominant role of the sympathetic nervous system and norepinephrine (Figs. 6 and 7; and see (59)).

316 ***Vasodilation is not attenuated in TG mouse femoral arteries***

317 ACh-induced vasodilation is impaired in human hypertension and in many animal hypertension
318 models (reviewed in (55)). Despite the modestly elevated basal BP in TG mice (Fig. 5A and (23)),
319 however, ACh-induced vasodilation of femoral arteries was comparable in TG and control mouse femoral
320 arteries (Fig. 11): the ACh-induced decline in arterial $[Ca^{2+}]_{CYT}$ and vasodilation, normalized to PD, were
321 virtually identical in control and TG mice (Figs. 11B, C). This implies that the endothelium-mediated
322 vasodilator mechanisms, including the release of NO, were not compromised in the TG mice despite the
323 chronic BP elevation. Although the PDs of TG mouse arteries were only slightly smaller than those of
324 the controls (Fig. 11 legend), a similar difference was seen when all arteries were averaged (Ctrl PD 397
325 ± 5 μM, n = 51; TG 380 ± 5; n = 51; P <0.03; data from experiments of Figs. 2, 6-8, 11 and 12).

326 Surprisingly, comparison of the vasodilation activated by the NO donor, SNP, in the two
327 phenotypes revealed that the TG mouse femoral arteries were significantly more sensitive to SNP than the
328 controls (Fig. 12). The TG artery diameter, normalized vasodilation and $\Delta[Ca^{2+}]_{CYT}$ SNP dose-response
329 curves were all shifted leftward (toward lower SNP doses) compared to controls (Fig. 11A-C). Thus,
330 although the endothelium-mediated vasodilator mechanisms apparently were normal (Fig. 11), either the
331 myocyte protein kinase G response to NO was enhanced, or some downstream vasodilator mechanism in
332 the ASMCs was up-regulated in the TG mice.

333

DISCUSSION

ASMC NCX1 preferentially mediates Ca^{2+} entry under basal conditions in vivo

NCX1, along with the plasma membrane Ca^{2+} pump (50) and various Ca^{2+}-permeable channels (16, 24) help to maintain Ca^{2+} homeostasis in ASMCs. NCX1 can mediate Ca^{2+} influx as well as efflux, and is important not only for clearing Ca^{2+} following Ca^{2+} transients (39, 41) but also for mediating net Ca^{2+} entry and maintaining elevated $[Ca^{2+}]_{CYT}$ during the development and maintenance of arterial tone (23, 44, 45, 61). The latter is exemplified by the observations that local inhibition of NCX1 modestly lowers basal arterial $[Ca^{2+}]_{CYT}$ and dilates tonically-constricted control arteries (Fig. 3B, C). Therefore it is not surprising that increasing NCX1 capacity by transgenic overexpression of NCX1 in smooth muscle (Fig. 1), increases basal $[Ca^{2+}]_{CYT}$ and arterial tone, and elevates BP (Fig. 2) (23). This demonstrates that NCX1 mediates Ca^{2+} entry in vivo under basal conditions.

To better understand these effects, the influence of vasoconstrictors and vasodilators on BP, and on femoral arteries in vivo (under anesthesia), was studied in control and smooth muscle-specific NCX1-TG mice. The homozygous TG/TG mice markedly overexpress NCX1 in arterial myocytes (Fig. 1) because of random insertion of the transgene into the genome. The overexpression was functionally confirmed by the augmented SEA0400-induced vasodilation and decline in $\Delta[Ca^{2+}]_{CYT}$ (Fig. 3), and the increase in ouabain-induced, SEA0400-sensitive vasoconstriction in the TG mouse arteries (Fig. 4).

Role of arterial NCX1 activity in the control of basal $[Ca^{2+}]_{CYT}$ and arterial tone

If NCX1 helps regulate $[Ca^{2+}]_{CYT}$ in ASMCs primarily by promoting Ca^{2+} entry (23, 62), and, if arterial constriction and tone depend on Ca^{2+} signals (13, 29, 60), it follows that knockout of myocyte NCX1 would be expected to lower $[Ca^{2+}]_{CYT}$, and reduce arterial tone and BP, as observed (44, 57, 62). Conversely, overexpression of NCX1 in ASMCs may be expected to raise $[Ca^{2+}]_{CYT}$, and augment arterial tone (Figs. 2, 3). Further, the elevated BP in TG mice (Fig. 5A) (23) fits with the inference that the role of NCX1 observed in muscular femoral arteries also applies to small resistance arteries with myogenic tone (57, 62).

The contribution of NCX1 to basal $[Ca^{2+}]_{CYT}$ and arterial tone is indicated by the effects of genetically-altered NCX1 expression and NCX1 blockade by SEA0400. The amplification of the effects of blockade in TG arteries (Fig. 3) and, especially, the absence of effects on arterial tone and BP in NCX1 knockout mice (57, 62), indicates the specificity of low-dose (0.3 μM) SEA0400 action. While the SEA0400-induced fall in $[Ca^{2+}]_{CYT}$ was significant, the 17% decline in control muscular artery basal tone did not reach statistical significance (Fig. 3). [Power analysis indicates that a far larger number of arteries would be required, given the small magnitude of the decrease and the variance of the measurements.] Nevertheless, the trend conforms to the similar, but statistically significant, ≈15% decrease in resistance artery myogenic tone previously observed in 0.3 μM SEA0400-treated isolated control arteries (23, 44). The SEA0400-induced changes indicate that NCX1 accounted for about 27% of basal $[Ca^{2+}]_{CYT}$ and about 19% of basal tone in TG mouse femoral arteries.

In a post hoc analysis following completion of all the experiments, the relationship between femoral artery $[Ca^{2+}]_{CYT}$ and tone was examined for the myriad conditions tested. The data (○, ▼ and Δ), shown as an in vivo (under light anesthesia) pCa vs arterial constriction plot in Fig. 13, reveal that constriction is nearly linearly related to $\log[Ca^{2+}]_{CYT}$ between 100 and 550 nM $[Ca^{2+}]_{CYT}$. The exMLCK FRET calibration data (58) are included in the figure (●). For comparison, a plot of pCa vs myogenic constriction in isolated, pressurized rat small cerebral arteries (29) is also shown (■) because myogenic tone in small arteries is directly related to intracellular $[Ca^{2+}]$ measured with fura-2 (13, 29). The inflection point (~120 nM $[Ca^{2+}]_{CYT}$; pCa = 6.92) is similar for the femoral and small cerebral arteries, presumably because this is close to the contraction threshold. However, the normalized small artery constriction curve is steeper than that for the femoral arteries, and reaches maximal constriction (diameter ≈ 40 μm) at $[Ca^{2+}]_{CYT} \simeq 325$ nM (pCa = 6.5). The larger arteries have a larger range of constriction (from ≈400 to ≈150 μm vs ≈200 to ≈40 μm for the small arteries) and are not yet maximally constricted at $[Ca^{2+}]_{CYT}$ = 550 nM (pCa = 6.26). This relationship implies that small NCX1-dependent changes in $[Ca^{2+}]_{CYT}$ may have a large effect on arterial constriction and BP. The evidence that control and TG

artery data fit the same curve implies that the sensitivity of the contractile apparatus to Ca^{2+} did not vary under the conditions examined here, consistent with the data in Figs. 6 and 8.

Dominant role of sympathetic drive in maintaining basal femoral artery tone

In contrast to the modest effects of SEA0400 in control mice, blockade of α1 adrenceptors with prazosin reduced femoral artery $[Ca^{2+}]_{CYT}$ by ≈65% and basal tone by ≈55% (Fig. 7). Blockade of sympathetic ganglia with hexamethonium reduced $[Ca^{2+}]_{CYT}$ and basal tone by ≥ 90% in control mice and by even more in TG mice (Figs. 8). Nevertheless, the data in Fig. 3 suggest that a modest fraction of the almost entirely SNA-driven tone (59), perhaps ≈15% in normal femoral arteries, also depends upon NCX1-mediated Ca^{2+} entry, but the majority apparently depends upon other Ca^{2+} transporters and channels. Basal $[Ca^{2+}]_{CYT}$ and tone in TG as well as control mouse arteries were, however, negligibly affected by the AT_1R inhibitor, losartan (Fig. 10), even though it effectively blocked Ang II-evoked $[Ca^{2+}]_{CYT}$ elevation and vasoconstriction (Fig. 9). These findings corroborate earlier reports that in vivo basal arterial tone in the mouse femoral arteries is largely determined by sympathetic drive (58, 59).

Why is Ang II-induced BP elevation greater in SM-NCX1-TG mice than in controls?

Ang II, whether infused acutely (iv) or chronically (sc), is widely known to increase BP (37, 48, 58). Interestingly, not only is basal BP modestly elevated in SM-NCX1-TG mice, but both acute and chronic Ang II induced a larger BP increment in TGs than in controls (Fig. 5). Conversely, SM-NCX1-KO mice are modestly hypotensive (57, 62) and the chronic Ang II-induced BP elevation tends to be smaller than in either control or TG mice (Fig. 5A). Thus, the Ang II-induced BP elevation appears to be arterial NCX1 'dose-dependent'.

The results summarized in the preceding paragraph might suggest that TG mouse arteries are more sensitive to vasoconstrictors than are control arteries. For example, if basal $[Ca^{2+}]_{CYT}$ is elevated, the SR Ca^{2+} stores and evoked Ca^{2+} signals might be expected to increase, but this apparently is not the case. Femoral arteries in anesthetized TG and control mice exhibited virtually identical vasoconstrictor responses (measured as 'Δ diameter') to locally superfused PE (Fig. 6) and Ang II (Fig. 9A). The

409 downward shift of the PE dose vs TG artery diameter curve (i.e., the dose-response curve), relative to the
410 control artery curve (Fig. 6A), implies that the PE constriction of TG arteries is superimposed on the
411 augmented basal constriction. The normalized curves (relative to PD; Fig. 6B) are nearly identical,
412 however, indicating that there is no difference in PE sensitivity (i.e., half-maximal activation or $K_{0.5}$)
413 between control and TG. It is noteworthy that a very similar result was obtained when PE-induced
414 femoral artery vasoconstriction was compared in controls and in mice infused chronically with Ang II to
415 induce hypertension (58).

416 Complementary effects were observed in SM-NCX1-KO mice which have low BP. Basal
417 myogenic tone was lower in KO than in control resistance arteries, and the PE dose-response curve was
418 simply displaced downward in the KOs (62). In vivo-infused Ang II dose-BP response data also indicate
419 that the curve for the KO mouse arteries paralleled that of controls but was displaced downward (63).
420 Thus, basal tone and BP are directly related to the level of NCX1 expression in control, TG and KO
421 arteries.

422 TG and control arteries also constricted to the same extent when tested with 100 nM Ang II (Fig.
423 9A). Furthermore, the amplitude of the Ang II-induced rise in $[Ca^{2+}]_{CYT}$ also was virtually identical in the
424 control and TG arteries (i.e., the signal, itself, was not amplified), but it was superimposed on a higher
425 basal $[Ca^{2+}]_{CYT}$ in the TG arteries (Fig. 9B). A possible explanation for the lack of signal amplification is
426 that compensatory mechanisms (e.g., reduced SERCA expression) might be triggered to minimize the
427 effects of the enhanced Ca^{2+} entry in TG mouse ASMCs; this needs verification. Importantly, our
428 measurements of $[Ca^{2+}]_{CYT}$ are spatial averages of cytoplasmic Ca^{2+}. We cannot eliminate the possibility
429 that overexpression of NCX1 changed $[Ca^{2+}]$ in other cellular compartments in which Ca^{2+} signaling
430 occurs, such as the endoplasmic reticulum or nuclear envelope. Thus, differences between control and
431 SM-NCX1-TG mice could, in ways yet unknown, be due also to changes in $[Ca^{2+}]$ in these compartments.

432 In contrast, femoral arteries of mice with Ang II-induced hypertension give attenuated $[Ca^{2+}]_{CYT}$
433 and vasoconstrictor responses to superfused Ang II, relative to controls (58). In that case, the sustained
434 elevation of plasma Ang II likely caused down-regulation of AT_1Rs (56) to compensate (partially) for the

hyper-stimulation. There is no reason to expect hyper-stimulation of either α1 adrenoceptors or AT_1Rs in NCX1-TG hypertension; consequently, agonist-induced down-regulation of the cognate receptors seems unlikely.

If TG arteries do not have enhanced sensitivity to vasoconstrictors, what accounts for the augmented BP elevation in TG mice, vs controls, when Ang II is infused (Fig. 5)? A likely explanation is based on the evidence that basal arterial diameter is smaller and arterial tone is greater not only in TG mouse muscular arteries than controls (Fig. 2) but, importantly, also in resistance arteries (unpublished) which account for most of the total peripheral resistance (TPR). Furthermore, artery resistance, R, is proportional to $1/r^4$, where r = artery radius (4). Under these circumstances, the same vasoconstrictor-induced artery diameter decrease in control and TG mice should cause a greater increase in TPR and BP in the TG mice (assuming constant cardiac output, CO, since BP = CO x TPR (4)). In other words, the vasoconstrictor-induced increase in TPR and, thus, in BP, is amplified in the TG mice simply because the increase is superimposed on a greater basal tone.

SNP-, but not ACh-induced vasodilation is enhanced in TG mouse arteries

Endothelium-dependent vasodilation, as measured with ACh stimulation (38), is often impaired in the arteries of hypertensive humans and animal models (55). One might anticipate, therefore, that ACh-induced vasodilation would be attenuated in TG mice with chronically elevated BP. On the contrary, the data in Fig. 11 reveal that the response of TG mouse arteries to ACh is normal. This implies that the endothelial impairment in hypertension may not simply be the result of the elevated intravascular pressure (19). When vasodilation was induced with SNP, however, the dose-response curve was shifted to the left in TG arteries; i.e., sensitivity to the NO donor was increased: the apparent EC_{50} was ~100 nM in controls, but only ~20 nM in the TG arteries (Fig. 11). This is not totally unexpected because there are reports that the sensitivity to SNP, largely an endothelium-independent vasodilator (for evidence of endothelium-dependent effects see (28)), is increased in some forms of hypertension (12, 52). In arterial myocytes, NO stimulates protein kinase G to increase the cyclic GMP level; this activates myosin light

chain phosphatase which promotes vasodilation by reducing myocyte sensitivity to Ca^{2+} (11), although other mechanisms may also contribute (33, 64). It seems possible that one or more of these vasodilator pathways was augmented to help compensate for the tendency of NCX1 overexpression to drive BP up. Indeed, others have suggested that Ca^{2+} sensitivity may be reduced in hypertension (1).

Conclusions

The aim of this in vivo study was to test the seemingly intuitive hypothesis that elevated arterial myocyte $[Ca^{2+}]_{CYT}$ and enhanced myocyte Ca^{2+} signaling can explain the mild hypertension in NCX1-TG mice. While TG mice have high basal $[Ca^{2+}]_{CYT}$ and enhanced arterial tone, the data indicate that the arterial myocytes are not hyper-sensitive to vasoconstrictors, as also has been reported for human small arteries (1, 51). Aalkjaer and colleagues (1) attributed the enhanced agonist-induced pressor response without a change in agonist sensitivity to "altered vascular structure" but "unchanged or possibly depressed" myocyte function. In contrast, however, the present results indicate that the increased pressor response in the TG-hypertensive mice is largely due to the superimposition of normal agonist-induced contraction on an artery with already enhanced basal tone. Despite the (presumably) congenitally high BP, the arterial functional responses appeared normal: the arteries constricted normally to PE and Ang II, and dilated to a PD that was only about 6-7% narrower than that of the controls in response to ACh and SNP. This suggests that there is relatively little structural remodeling (21, 31) of the TG arteries despite longstanding hypertension. Thus, at least in NCX1-TG hypertension, the primary defect appears to be the NCX1-mediated elevation of $[Ca^{2+}]_{CYT}$ and its functional consequences, most notably, enhanced basal tone, that lead directly to increased TPR. Because arterial NCX1 is up-regulated in many forms of hypertension (10, 42, 43, 65), it seems reasonable to anticipate that similar functional (active contraction) changes likely also apply at least during the early stages of the hypertension. We also made the unexpected observation that endothelial function is not attenuated in the femoral arteries of modestly hypertensive SM-NCX1-TG mice (Fig. 11), and that vasodilator mechanisms are even augmented (Fig.

12). These observations seem inconsistent with the popular view that BP elevation, per se, impairs endothelium-dependent vasodilation (35).

The key observation is that, while sympathetic drive is the dominant mechanism responsible for sustaining arterial tone, Ca^{2+} entry via NCX1 plays a small but crucial role in helping to maintain $[Ca^{2+}]_{CYT}$ above contraction threshold. The critical relationship between $[Ca^{2+}]_{CYT}$ and arterial tone (Fig. 13) illustrates how enhanced net NCX1-mediated Ca^{2+} entry can increase tone. Net Ca^{2+} transport by NCX1 is governed by the PM Na^+ electrochemical gradient (Introduction and (9)) that is controlled by adjacent $\alpha 2$ Na^+ pumps in myocyte PLasmERosomes (Introduction and (8, 27, 39)). Apparently, $\alpha 2$ Na^+ pump activity is ultimately responsible for modulating arterial tone, TPR and BP through NCX1 (7). The steep relationship between $[Ca^{2+}]_{CYT}$ and arterial tone (Fig. 13) suggests that very modest increases in SNA (40) and plasma endogenous ouabain (5, 20), which increases arterial NCX1 expression (43, 66), may act in concert to elevate BP in many forms of hypertension.

Acknowledgements

We thank Ms. Meng Li for maintaining the mouse colony and for laboratory support and Prof. Soren Bentzen for advice and assistance with statistical analyses. Supported by funds from the National Institutes of Health/NHLBI (R01HL107654 to WGW; R01 HL-45215 and R01 HL-107555 to MPB), the American Heart Association (15GRNT24940022 to JZ and then to MPB), the National Natural Science Foundation of China (Grant No. 81100174 and 81570449 to YW), the Fundamental Research Funds for the Central Universities (No. GK201803097 to YW), the College Students' Innovative and Training Project of Shaanxi Normal University (No. cx2018197 to YW), and the University of Maryland Baltimore Foundation (Center for Heart Hypertension & Kidney Diseases Fund). The work was also supported by the University of Maryland School of Medicine Physiological Phenotyping Core (LC, Core Manager).

Disclosures

No conflicts of interest, financial or otherwise, are declared by the authors.

References

1. **Aalkjaer C, Heagerty AM, Petersen KK, Swales JD, and Mulvany MJ**. Evidence for increased media thickness, increased neuronal amine uptake, and depressed excitation--contraction coupling in isolated resistance vessels from essential hypertensives. *Circ Res* 61: 181-186, 1987.
2. **Aalkjaer C, and Mulvany MJ**. Sodium metabolism in rat resistance vessels. *J Physiol* 343: 105-116, 1983.
3. **Baryshnikov SG, Pulina MV, Zulian A, Linde CI, and Golovina VA**. Orai1, a critical component of store-operated Ca^{2+} entry, is functionally associated with Na^+/Ca^{2+} exchanger and plasma membrane Ca^{2+} pump in proliferating human arterial myocytes. *Am J Physiol Cell Physiol* 297: C1103-1112, 2009.
4. **Berne RM, and Levy MN**. *Cardiovascular Physiology*. St. Louis, MO: Mosby, 2001, p. 115-153.
5. **Blaustein MP**. The pump, the exchanger, and the holy spirit: origins and 40-year evolution of ideas about the ouabain-Na^+ pump endocrine system. *Am J Physiol Cell Physiol* 314: C3-C26, 2018.
6. **Blaustein MP**. Sodium ions, calcium ions, blood pressure regulation, and hypertension: a reassessment and a hypothesis. *Am J Physiol Cell Physiol* 232: C165-C173, 1977.
7. **Blaustein MP, Chen L, Hamlyn JM, Leenen FH, Lingrel JB, Wier WG, and Zhang J**. Pivotal role of $\alpha 2$ Na^+ pumps and their high affinity ouabain binding site in cardiovascular health and disease. *J Physiol* 594: 6079-6103, 2016.
8. **Blaustein MP, Juhaszova M, and Golovina VA**. The cellular mechanism of action of cardiotonic steroids: a new hypothesis. *Clin Exp Hypertens* 20:: 691-703, 1998.
9. **Blaustein MP, and Lederer WJ**. Sodium/calcium exchange: its physiological implications. *Physiol Rev* 79: 763-854, 1999.
10. **Blaustein MP, Leenen FH, Chen L, Golovina VA, Hamlyn JM, Pallone TL, Van Huysse JW, Zhang J, and Wier WG**. How NaCl raises blood pressure: a new paradigm for the pathogenesis of salt-dependent hypertension. *Am J Physiol Heart Circ Physiol* 302: H1031-1049, 2012.
11. **Bolz SS, Vogel L, Sollinger D, Derwand R, de Wit C, Loirand G, and Pohl U**. Nitric oxide-induced decrease in calcium sensitivity of resistance arteries is attributable to activation of the myosin light chain phosphatase and antagonized by the RhoA/Rho kinase pathway. *Circulation* 107: 3081-3087, 2003.
12. **Cohen DM, Webb RC, and Bohr DF**. Nitroprusside-induced vascular relaxation in DOCA hypertensive rats. *Hypertension* 4: 13-19, 1982.
13. **D'Angelo G, Davis MJ, and Meininger GA**. Calcium and mechanotransduction of the myogenic response. *Am J Physiol Heart Circ Physiol* 273: H175-182, 1997.
14. **Dostanic-Larson I, Van Huysse JW, Lorenz JN, and Lingrel JB**. The highly conserved cardiac glycoside binding site of Na,K-ATPase plays a role in blood pressure regulation. *Proc Natl Acad Sci USA* 102: 15845-15850, 2005.
15. **Dostanic I, Paul RJ, Lorenz JN, Theriault S, Van Huysse JW, and Lingrel JB**. The α_2-isoform of Na-K-ATPase mediates ouabain-induced hypertension in mice and increased vascular contractility in vitro. *Am J Physiol Heart Circ Physiol* 288: H477-H485, 2005.
16. **Earley S, and Brayden JE**. Transient receptor potential channels in the vasculature. *Physiol Rev* 95: 645-690, 2015.
17. **Folkow B, and Neil E**. *Circulation*. New York: Oxford University Press, 1971, p. 593.
18. **Geguchadze R, Zhi G, Lau KS, Isotani E, Persechini A, Kamm KE, and Stull JT**. Quantitative measurements of Ca^{2+}/calmodulin binding and activation of myosin light chain kinase in cells. *FEBS Lett* 557: 121-124, 2004.
19. **Gunduz F, Baskurt OK, and Meiselman HJ**. Vascular dilation responses of rat small mesenteric arteries at high intravascular pressure in spontaneously hypertensive rats. *Circ J* 73: 2091-2097, 2009.

20. **Hamlyn JM, and Blaustein MP**. Endogenous Ouabain: Recent Advances and Controversies. *Hypertension* 68: 526-532, 2016.
21. **Heagerty AM, Aalkjaer C, Bund SJ, Korsgaard N, and Mulvany MJ**. Small artery structure in hypertension. Dual processes of remodeling and growth. *Hypertension* 21: 391-397, 1993.
22. **Isotani E, Zhi G, Lau KS, Huang J, Mizuno Y, Persechini A, Geguchadze R, Kamm KE, and Stull JT**. Real-time evaluation of myosin light chain kinase activation in smooth muscle tissues from a transgenic calmodulin-biosensor mouse. *Proc Natl Acad Sci USA* 101: 6279-6284, 2004.
23. **Iwamoto T, Kita S, Zhang J, Blaustein MP, Arai Y, Yoshida S, Wakimoto K, Komuro I, and Katsuragi T**. Salt-sensitive hypertension is triggered by Ca^{2+} entry via Na^+/Ca^{2+} exchanger type-1 in vascular smooth muscle *Nature Med* 10: 1193-1199, 2004.
24. **Jaggar JH, Wellman GC, Heppner TJ, Porter VA, Perez GJ, Gollasch M, Kleppisch T, Rubart M, Stevenson AS, Lederer WJ, Knot HJ, Bonev AD, and Nelson MT**. Ca^{2+} channels, ryanodine receptors and Ca^{2+}-activated K^+ channels: a functional unit for regulating arterial tone. *Acta Physiol Scand* 164: 577-587, 1998.
25. **Janssen BJ, De Celle T, Debets JJ, Brouns AE, Callahan MF, and Smith TL**. Effects of anesthetics on systemic hemodynamics in mice. *Am J Physiol Heart Circ Physiol* 287: H1618-H1624, 2004.
26. **Jones AW**. Electrolyte metabolism of the arterial wall. In: *Vascular Smooth Muscle: Metabolic, Ionic and Contractile Mechanisms*, edited by Crass MF, III, and Barnes, C.D. New York: Academic Press, 1982, p. 37-70.
27. **Juhaszova M, and Blaustein MP**. Distinct distribution of different Na^+ pump alpha subunit isoforms in plasmalemma. Physiological implications. *Ann NY Acad Sci* 834: 524-536, 1997.
28. **Kangussu LM, Olivon VC, Arifa RD, Araujo N, Reis D, Assis MT, Soriani FM, de Souza Dda G, Bendhack LM, and Bonaventura D**. Enhancement on reactive oxygen species and COX-1 mRNA levels modulate the vascular relaxation induced by sodium nitroprusside in denuded mice aorta. *Fundam Clin Pharmacol* 29: 150-163, 2015.
29. **Knot HJ, and Nelson MT**. Regulation of arterial diameter and wall Ca^{2+} in cerebral arteries of rat by membrane potential and intravascular pressure. *J Physiol* 508 199-209, 1998.
30. **Kokita N, Stekiel TA, Yamazaki M, Bosnjak ZJ, Kampine JP, and Stekiel WJ**. Potassium channel-mediated hyperpolarization of mesenteric vascular smooth muscle by isoflurane. *Anesthesiology* 90: 779-788, 1999.
31. **Korsgaard N, Aalkjaer C, Heagerty AM, Izzard AS, and Mulvany MJ**. Histology of subcutaneous small arteries from patients with essential hypertension. *Hypertension* 22: 523-526, 1993.
32. **Kotecha N, and Hill MA**. Myogenic contraction in rat skeletal muscle arterioles: smooth muscle membrane potential and Ca^{2+} signaling. *Am J Physiol Heart Circ Physiol* 289: H1326-1334, 2005.
33. **Kyle BD, Mishra RC, and Braun AP**. The augmentation of BK channel activity by nitric oxide signaling in rat cerebral arteries involves co-localized regulatory elements. *J Cereb Blood Flow Metab* 37: 3759-3773, 2017.
34. **Linde CI, Antos LK, Golovina VA, and Blaustein MP**. Nanomolar ouabain increases NCX1 expression and enhances Ca^{2+} signaling in human arterial myocytes: a mechanism that links salt to increased vascular resistance? *Am J Physiol Heart Circ Physiol* 303: H784-794, 2012.
35. **Lockette W, Otsuka Y, and Carretero O**. The loss of endothelium-dependent vascular relaxation in hypertension. *Hypertension* 8: II61-66, 1986.
36. **Lorenz JN, Loreaux EL, Dostanic-Larson I, Lasko V, Schnetzer JR, Paul RJ, and Lingrel JB**. ACTH-induced hypertension is dependent on the ouabain-binding site of the α_2-Na^+-K^+-ATPase subunit. *Am J Physiol Heart Circ Physiol* 295: H273-280, 2008.
37. **Luft FC, Wilcox CS, Unger T, Kuhn R, Demmert G, Rohmeiss P, Ganten D, and Sterzel RB**. Angiotensin-induced hypertension in the rat. Sympathetic nerve activity and prostaglandins. *Hypertension* 14: 396-403, 1989.

606 38. **Luscher TF, Raij L, and Vanhoutte PM**. Endothelium-dependent vascular responses in
607 normotensive and hypertensive Dahl rats. *Hypertension* 9: 157-163, 1987.
608 39. **Lynch RM, Weber CS, Nullmeyer KD, Moore ED, and Paul RJ**. Clearance of store-released Ca^{2+}
609 by the Na^+-Ca^{2+} exchanger is diminished in aortic smooth muscle from Na^+-K^+-ATPase α_2-isoform gene-
610 ablated mice. *Am J Physiol Heart Circ Physiol* 294: H1407-H1416, 2008.
611 40. **Mark AL**. Regulation of sympathetic nerve activity in mild human hypertension. *J Hypertens*
612 *Suppl* 8: S67-75, 1990.
613 41. **Pritchard TJ, Bowman PS, Jefferson A, Tosun M, Lynch RM, and Paul RJ**. Na^+-K^+-ATPase and Ca^{2+}
614 clearance proteins in smooth muscle: a functional unit. *Am J Physiol Heart Circ Physiol* 299: H548-556,
615 2010.
616 42. **Pulina MV, Zulian A, Baryshnikov SG, Linde CI, Karashima E, Hamlyn JM, Ferrari P, Blaustein**
617 **MP, and Golovina VA**. Cross talk between plasma membrane Na^+/Ca^{2+} exchanger-1 and TRPC/Orai-
618 containing channels: key players in arterial hypertension. *Adv Exp Med Biol* 961: 365-374, 2013.
619 43. **Pulina MV, Zulian A, Berra-Romani R, Beskina O, Mazzocco-Spezzia A, Baryshnikov SG,**
620 **Papparella I, Hamlyn JM, Blaustein MP, and Golovina VA**. Upregulation of Na^+ and Ca^{2+} transporters in
621 arterial smooth muscle from ouabain-induced hypertensive rats. *Am J Physiol Heart Circ Physiol* 298:
622 H263-274, 2010.
623 44. **Raina H, Ella SR, and Hill MA**. Decreased activity of the smooth muscle Na^+/Ca^{2+} exchanger
624 impairs arteriolar myogenic reactivity. *J Physiol* 586: 1669-1681, 2008.
625 45. **Rebolledo A, Speroni F, Raingo J, Salemme SV, Tanzi F, Munin V, Anon MC, and Milesi V**. The
626 Na^+/Ca^{2+} exchanger is active and working in the reverse mode in human umbilical artery smooth muscle
627 cells. *Biochem Biophys Res Commun* 339: 840-845, 2006.
628 46. **Reuter H, Blaustein MP, and Haeusler G**. Na-Ca exchange and tension development in arterial
629 smooth muscle. *Philos Trans R Soc Lond B Biol Sci* 265: 87-94, 1973.
630 47. **Rüegg JC**. *Calcium in Muscle Contraction: Cellular and Molecular Physiology*. Berlin: Springer-
631 Verlag 1992, pp. 206-212.
632 48. **Saxena PR**. Interaction between the renin-angiotensin-aldosterone and sympathetic nervous
633 systems. *J Cardiovasc Pharmacol* 19 Suppl 6: S80-88, 1992.
634 49. **Seagard JL, Hopp FA, Bosnjak ZJ, Osborn JL, and Kampine JP**. Sympathetic efferent nerve
635 activity in conscious and isoflurane-anesthetized dogs. *Anesthesiology* 61: 266-270, 1984.
636 50. **Shimizu H, Borin ML, and Blaustein MP**. Use of La^{3+} to distinguish activity of the plasmalemmal
637 Ca^{2+} pump from Na^+/Ca^{2+} exchange in arterial myocytes. *Cell Calcium* 21: 31-41, 1997.
638 51. **Sivertsson R**. The hemodynamic importance of structural vascular changes in essential
639 hypertension. *Acta Physiol Scand Suppl* 343: 1-56, 1970.
640 52. **Tesfamariam B, and Halpern W**. Endothelium-dependent and endothelium-independent
641 vasodilation in resistance arteries from hypertensive rats. *Hypertension* 11: 440-444, 1988.
642 53. **Ullman J, Hargestam R, Lindahl S, Chan SH, Eriksson S, and Rundgren M**. Circulatory effects of
643 angiotensin II during anaesthesia, evaluated by real-time spectral analysis. *Acta Anaesthesiol Scand* 47:
644 532-540, 2003.
645 54. **van Breemen C, Chen Q, and Laher I**. Superficial buffer barrier function of smooth muscle
646 sarcoplasmic reticulum. *Trends Pharmacol Sci* 16: 98-105, 1995.
647 55. **Vanhoutte PM, Shimokawa H, Feletou M, and Tang EH**. Endothelial dysfunction and vascular
648 disease - a 30th anniversary update. *Acta Physiol* 219: 22-96, 2017.
649 56. **Wang DH, Du Y, and Yao A**. Regulation of the gene-encoding angiotensin II receptor in vascular
650 tissue. *Microcirculation* 3: 237-239, 1996.
651 57. **Wang Y, Chen L, Li M, Cha H, Iwamoto T, and Zhang J**. Conditional knockout of smooth muscle
652 sodium calcium exchanger type-1 lowers blood pressure and attenuates Angiotensin II-salt
653 hypertension. *Physiol Rep* 3: e12273,12210.14814/phy12272.12273, 2015.

58. **Wang Y, Chen L, Wier WG, and Zhang J**. Intravital Förster resonance energy transfer imaging reveals elevated $[Ca^{2+}]_i$ and enhanced sympathetic tone in femoral arteries of angiotensin II-infused hypertensive biosensor mice. *J Physiol* 591: 5321-5336, 2013.
59. **Zacharia J, Mauban JR, Raina H, Fisher SA, and Wier WG**. High vascular tone of mouse femoral arteries in vivo is determined by sympathetic nerve activity via α1A- and α1D-adrenoceptor subtypes. *PloS one* 8: e65969, 2013.
60. **Zhang J, Chen L, Raina H, Blaustein MP, and Wier WG**. In vivo assessment of artery smooth muscle $[Ca^{2+}]_i$ and MLCK activation in FRET-based biosensor mice. *Am J Physiol Heart Circ Physiol* 299: H946-956, 2010.
61. **Zhang J, Lee MY, Cavalli M, Chen L, Berra-Romani R, Balke CW, Bianchi G, Ferrari P, Hamlyn JM, Iwamoto T, Lingrel JB, Matteson DR, Wier WG, and Blaustein MP**. Sodium pump α2 subunits control myogenic tone and blood pressure in mice. *J Physiol* 569: 243-256, 2005.
62. **Zhang J, Ren C, Chen L, Navedo MF, Antos LK, Kinsey SP, Iwamoto T, Philipson KD, Kotlikoff MI, Santana LF, W.G. W, Matteson DR, and Blaustein MP**. Knockout of Na^+/Ca^{2+} exchanger in smooth muscle attenuates vasoconstriction and L-type Ca^{2+} channel current and lowers blood pressure. *Am J Physiol Heart Circ Physiol* 298: H1472-H1483, 2010.
63. **Zhao D, Zhang J, Blaustein MP, and Navar LG**. Attenuated renal vascular responses to acute angiotensin II infusion in smooth muscle-specific Na^+/Ca^{2+} exchanger knockout mice. *Am J Physiol Renal Physiol* 301: F574-579, 2011.
64. **Zhao Y, Vanhoutte PM, and Leung SW**. Vascular nitric oxide: Beyond eNOS. *J Pharmacol Sci* 129: 83-94, 2015.
65. **Zulian A, Baryshnikov SG, Linde CI, Hamlyn JM, Ferrari P, and Golovina VA**. Upregulation of $Na^{+/}Ca^{2+}$ exchanger and TRPC6 contributes to abnormal Ca^{2+} homeostasis in arterial smooth muscle cells from Milan hypertensive rats. *Am J Physiol Heart Circ Physiol* 299: H624-633, 2010.
66. **Zulian A, Linde CI, Pulina MV, Baryshnikov SG, Papparella I, Hamlyn JM, and Golovina VA**. Activation of c-SRC underlies the differential effects of ouabain and digoxin on Ca^{2+} signaling in arterial smooth muscle cells. *Am J Physiol Cell Physiol* 304: C324-C333, 2013.

683 **Figure Legends**

684 **Fig. 1.** NCX1 is overexpressed in smooth muscle-specific NCX1-transgenic mice. Immunoblot of de-
685 endothelialized aortic membrane proteins from control (Ctrl), and heterozygous and homozygous SM-
686 NCX1-TG mice (TG/+ and TG/TG, respectively). TG/TG mice were used for all physiological
687 experiments in this study. The NCX1 transgene was randomly inserted into the genome and the protein
688 was therefore greatly overexpressed, as illustrated. The protein samples had to be markedly diluted so
689 that both the control and TG NCX1 bands could be visualized on the same gel (also see Fig. S3 in (23)).
690 β-Actin was used for the loading control.

691 **Fig. 2.** Effects of smooth muscle-specific NCX1 overexpression on femoral artery $[Ca^{2+}]_{CYT}$, diameter
692 and tone. **(**A) Baseline diameter and passive diameter (PD), (B) basal tone (PD minus baseline diameter
693 as a % of PD), and (C) basal $[Ca^{2+}]_{CYT}$ in the exposed femoral arteries of Ctrl and TG mice in vivo, under
694 light anesthesia. Baseline diameter was reduced, and basal tone and $[Ca^{2+}]_{CYT}$ were increased in TG
695 mouse arteries. * = P<0.05 vs Ctrl (Student's unpaired t-test); *** = P<0.001 vs Ctrl and ### = P<0.001
696 vs the respective basal diameter (2-way ANOVA with pairwise comparisons using the Holm-Sidak
697 method). Numbers of Ctrl and TG mice are shown in parentheses at the top. The difference between the
698 mean Ctrl PD and TG PD was not significant (P = 0.085; 2-way ANOVA). When the mean PD values
699 from 6 independent experiments (with 51 Ctrl and 51 TG arteries) were analyzed, however, the respective
700 means of the means from each experiment (Ctrl PD = 397.2 ± 3.9 μm and TG PD = 379.5 ± 5.3 μm) were
701 significantly different (P = 0.023; Student's unpaired t-test). The 95% confidence interval for the
702 difference of the means was 3.043 to 32.291; the power of the t-test was 0.617.

703 **Fig. 3.** Effects of 0.3 μM SEA0400 on basal $[Ca^{2+}]_{CYT}$ (A) and basal tone (B) in Ctrl and TG femoral
704 arteries in vivo. The SEA0400-induced decrease in $[Ca^{2+}]_{CYT}$ ($\Delta[Ca^{2+}]_{CYT}$) and vasodilation (diameter
705 increase as % of PD) are also shown (B and D, respectively). The effects of SEA0400 were augmented in
706 TG mouse arteries. Statistics: 2-way ANOVA; * = P<0.05 vs the respective Ctrl; # = P<0.05 and ## =
707 P<0.01 vs basal TG; Δ = P<0.05 vs basal TG. Numbers of mice are in parentheses.

708 **Fig. 4.** Effects of ouabain and SEA0400 on femoral artery $[Ca^{2+}]_{CYT}$ and diameter. (A) $[Ca^{2+}]_{CYT}$ increase
709 ($\Delta[Ca^{2+}]_{CYT}$) and (B) vasoconstriction (diameter decrease, as a % of PD) induced by a 15 min superfusion
710 with 10 μM ouabain, and the effects of 0.3 μM SEA0400 on these changes. The ouabain-induced,
711 SEA0400-sensitive effects were amplified in TG mouse arteries. Statistics: paired T-test; # = P<0.05 vs
712 ouabain alone. Numbers of mice are in parentheses.

Fig.5. The acute and chronic Ang II-induced BP elevation is augmented in TG mouse arteries. A. Mean blood pressure (24 hr MBP) in awake, mobile SM-NCX1-KO (KO), Ctrl, and SM-NCX1-TG (TG) mice infused with saline- or Ang II (400 ng/kg/min, sc) for 3 weeks. B. Increases in aortic MBP (ΔMBP) induced by acute iv infusion of 30 or 300 ng/kg Ang II in lightly anesthetized KO, Ctrl and TG mice. Statistics: 2-way ANOVA; * = $P<0.05$; *** = $P<0.001$ for the pairs indicated. Numbers of mice are in parentheses.

Fig. 6. Phenylephrine (PE) cumulative dose-response curves for exposed femoral arteries in Ctrl and TG mice in vivo; the PE was applied by superfusion. A. PE dose vs artery diameter; Ctrl PD = 404±21 μm (n = 9); TG PD = 374±5 μm (n = 11). B. PE-induced vasoconstriction (as a % of PD). C. PE-induced increase (Δ) in $[Ca^{2+}]_{CYT}$. Basal $[Ca^{2+}]_{CYT}$ was 221 ± 29 nM in Ctrl and 319 ± 36 nM in TG mouse arteries, but the normalized vasoconstriction curves (B) and $[Ca^{2+}]_{CYT}$ curves (C) from Ctrl and TG mice are virtually superimposable (2-way ANOVA).

Fig. 7. Effects of α1-adrenergic blockade (prazosin) on femoral artery $[Ca^{2+}]_{CYT}$, diameter and tone in femoral arteries of control and SM-specific NCX1 overexpression (TG) mice. A. Diameters of exposed femoral arteries of Ctrl and TG mice in vivo, and the effects of superfusion with 300 nM and 1 μM prazosin. PD (arteries superfused with Ca^{2+}-free medium) is also shown; Ctrl PD = 403±13 μm (n = 6); TG PD = 397±12 μm (n = 6). B, C. $[Ca^{2+}]_{CYT}$ (B) and arterial tone (as % of PD; C) in Ctrl and TG mouse arteries under basal conditions and during superfusion with 300 nM prazosin. Prazosin reduced $[Ca^{2+}]_{CYT}$ and tone to a greater extent in TG than in Ctrl mice. Statistics: 2-way ANOVA; * = $P<0.05$, ** = $P<0.01$, *** = $P<0.001$ vs basal Ctrl; ## = $P<0.01$, ### = $P<0.001$ vs basal TG. Numbers of mice are in parentheses.

Fig. 8. Effects of iv injection of 3 mg/kg hexamethonium on arterial diameter (A; representative original recording) and mean arterial tone (B), and on $[Ca^{2+}]_{CYT}$ representative original data (C) and mean data (D) in exposed femoral arteries of Ctrl and WT mice in vivo. Hexamethonium redued $[Ca^{2+}]_{CYT}$ to <<50 nM and virtually abolished tone in both Ctrl and TG arteries. Ctrl PD = 382±14 μm (n = 8); TG PD = 386±12 μm (n = 8). Statistics: 2-way ANOVA; * = $P<0.05$, *** = $P<0.001$ vs basal Ctrl; ### = $P<0.001$ vs basal TG. Numbers of mice are in parentheses.

Fig. 9. Effects of superfusing 100 nM Ang II ± 100 nM losartan on the diameter (A), $[Ca^{2+}]_{CYT}$ (B) and tone (C; as % of PD) of exposed femoral arteries in Ctrl and WT mice in vivo. Losartan abolished nearly all of the Ang II-induced increases in $[Ca^{2+}]_{CYT}$ and tone in both Ctrl and TG arteries. Statistics: 2-way

ANOVA: *** = $P<0.001$ vs respective Ctrl or TG basal; ## = $P<0.01$ vs Ang II alone; Δ = $P<0.05$ vs Ctrl basal. Numbers of mice are in parentheses.

Fig. 10. Effects of superfusion with 100 nM losartan on the diameter (A), $[Ca^{2+}]_{CYT}$ (B) and tone (C; as % of PD) on exposed femoral arteries in Ctrl and WT mice in vivo. Losartan had negligible effect on $[Ca^{2+}]_{CYT}$ and tone in both Ctrl and TG arteries. Statistics: 2-way ANOVA; * = $P<0.05$ vs basal Ctrl. Numbers of mice are in parentheses.

Fig. 11. Acetylcholine (ACh) cumulative dose-response curves for exposed femoral arteries in Ctrl and TG mice in vivo; the ACh was applied by superfusion. A. ACh dose vs artery diameter; Ctrl PD = 390±19 μm (n = 6); TG PD = 361±16 μm (n = 10). B. PE-induced vasodilation (as a % of PD). C. ACh-induced decrease (Δ) in $[Ca^{2+}]_{CYT}$. Basal $[Ca^{2+}]_{CYT}$ was 230 ± 23 nM in Ctrl and 335 ± 10 nM in TG mouse arteries, but the normalized vasodilation curves (B) and $[Ca^{2+}]_{CYT}$ curves (C) from Ctrl and TG mice are virtually superimposable (2-way ANOVA).

Fig. 12. Sodium nitroprusside (SNP) cumulative dose-response curves for exposed femoral arteries in Ctrl and TG mice in vivo; the SNP was applied by superfusion. A. SNP dose vs artery diameter; Ctrl PD = 407±23 μm (n = 6); TG PD = 387±13 μm (n = 6). B. SNP-induced vasodilation (as a % of PD). C. SNP-induced decrease (Δ) in $[Ca^{2+}]_{CYT}$. Basal $[Ca^{2+}]_{CYT}$ was 219 ± 31 nM in Ctrl and 309 ± 27 nM in TG mouse arteries. The TG curves are all significantly shifted to the left (lower SNP EC_{50}'s) relative to the respective Ctrl curves (* = $P<0.05$). Statistics: 2-way ANOVA. Numbers of mice are in parentheses.

Fig. 13. Femoral artery constriction (% of PD) in vivo graphed as a function of pCa ($-\log[Ca^{2+}]_{CYT}$). The data were taken from Figs. 2-12 (○ = Ctrl; ▼ = TG) and from (58) (Δ). The regression lines for the three sets of data, for $[Ca^{2+}]_{CYT}$ = 100-500 nM (R = 0.91, 0.69 and, 0.97, respectively) were indistinguishable, and correspond to a constriction of approximately 10% of PD per 100 nM increase in $[Ca^{2+}]_{CYT}$. For comparison, the myogenic constriction vs pCa data in isolated, pressurized (60 mm Hg) rat small posterior cerebral arteries taken from Fig. 10 of (29)) are also shown (■); the constriction, as a % of PD was calculated based on a PD of 210 μm. The graph also contains the normalized exMLCK FRET ratio curve (●; where 0 = "0" $[Ca^{2+}]_{CYT}$; 100 = saturating $[Ca^{2+}]_{CYT}$) from Fig. 1B of (58).

Fig. 1

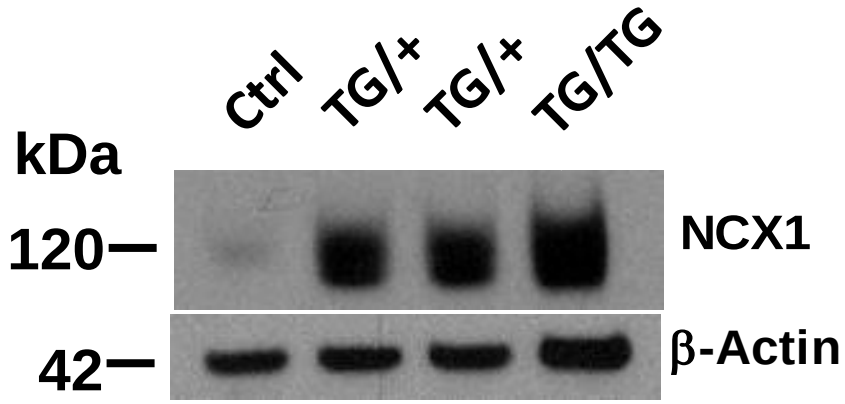

Fig. 2

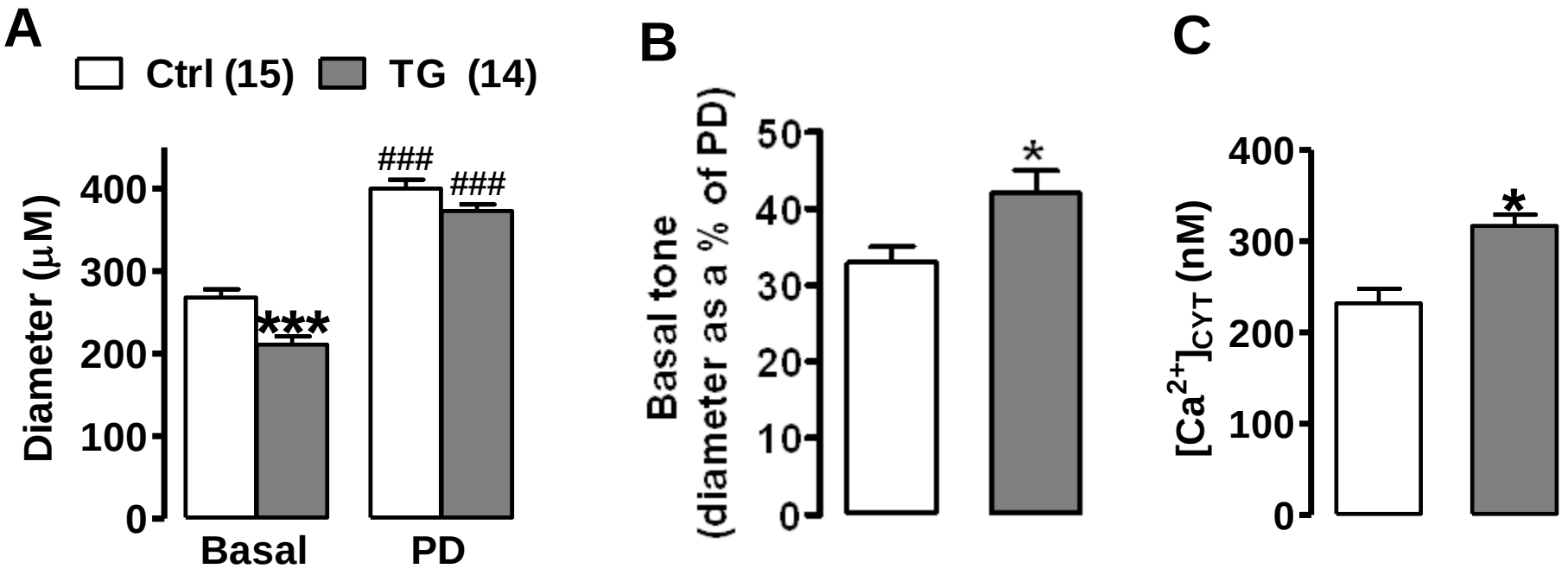

Fig. 3

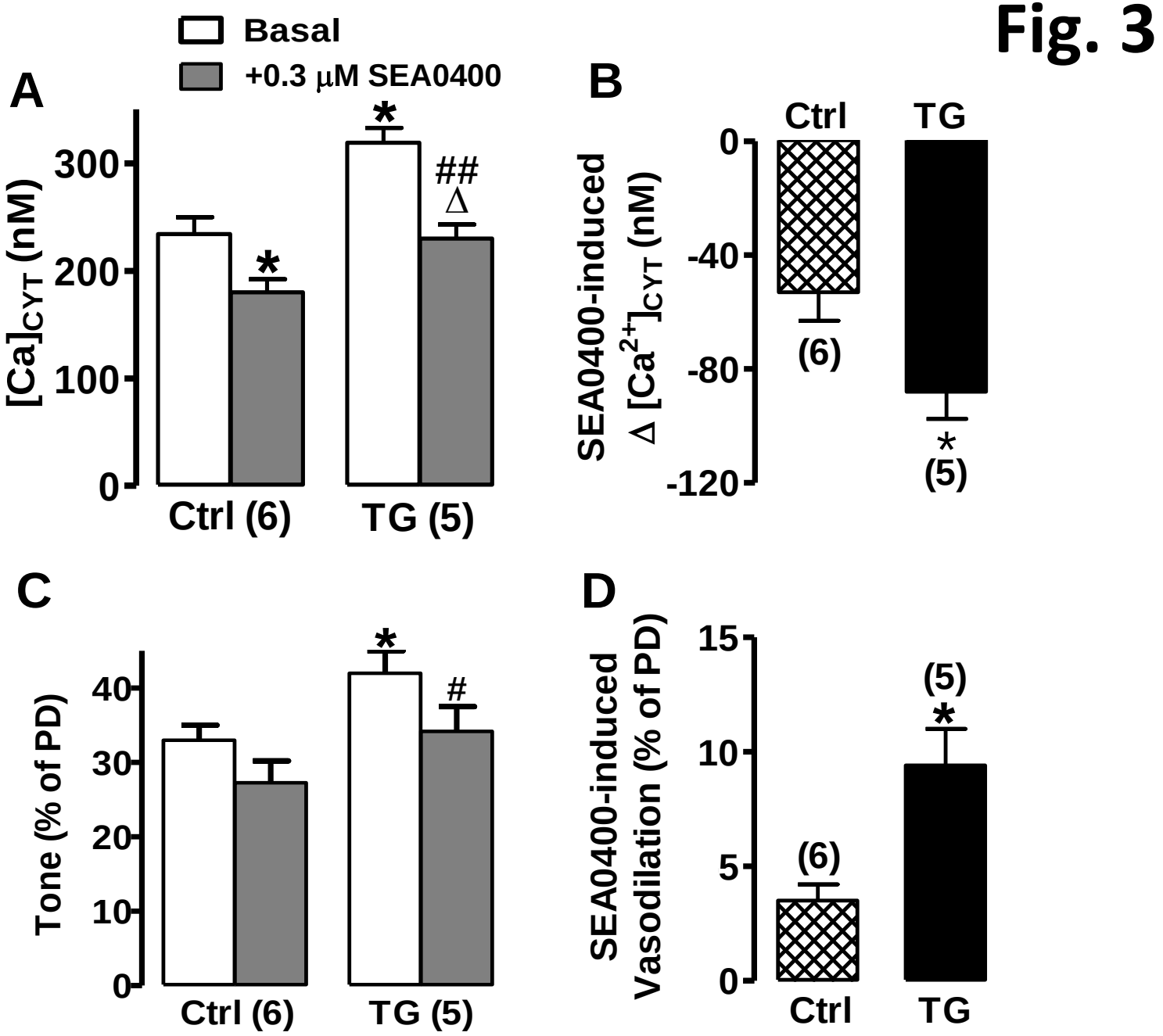

Fig. 4

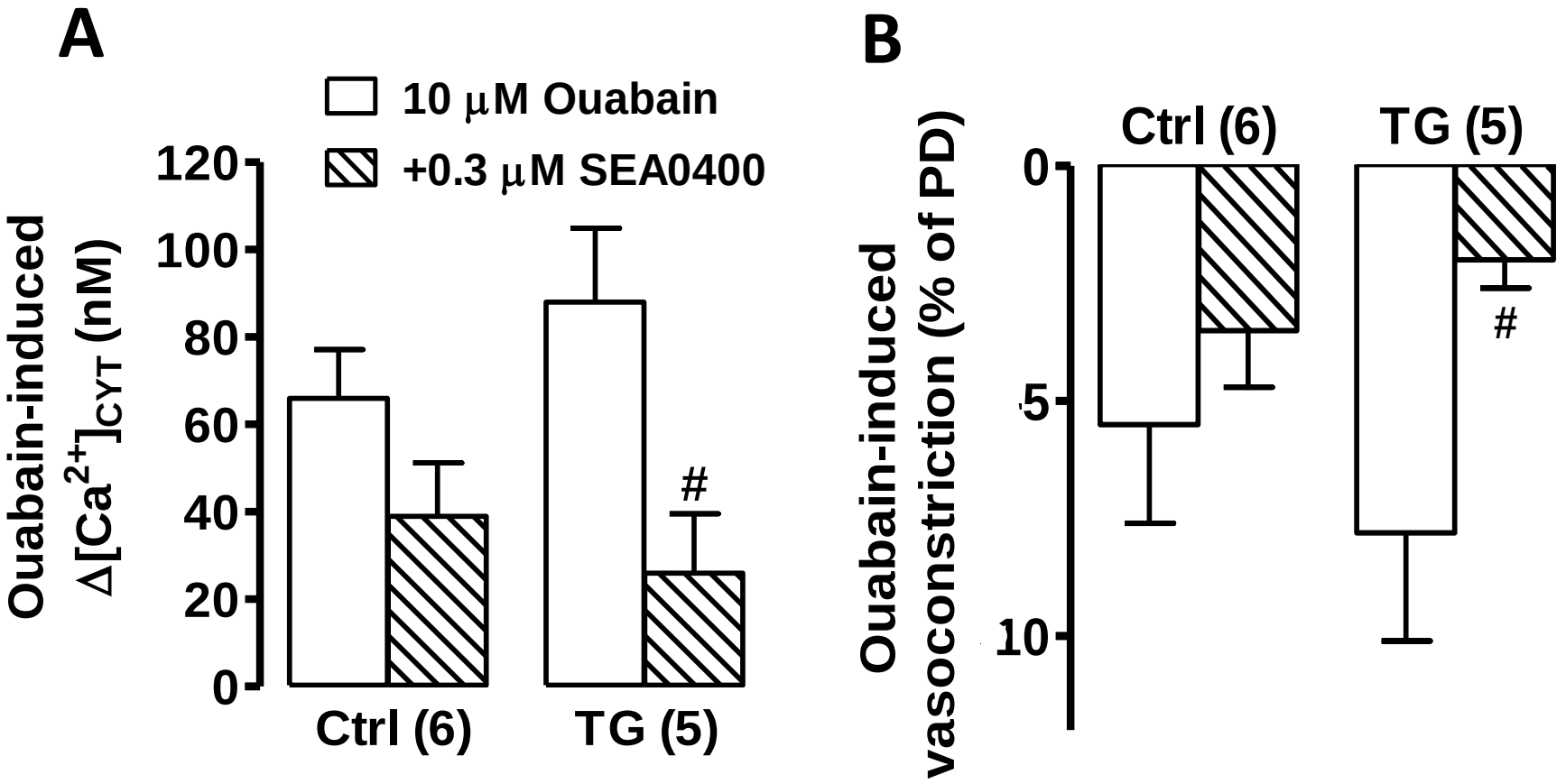

Fig. 5

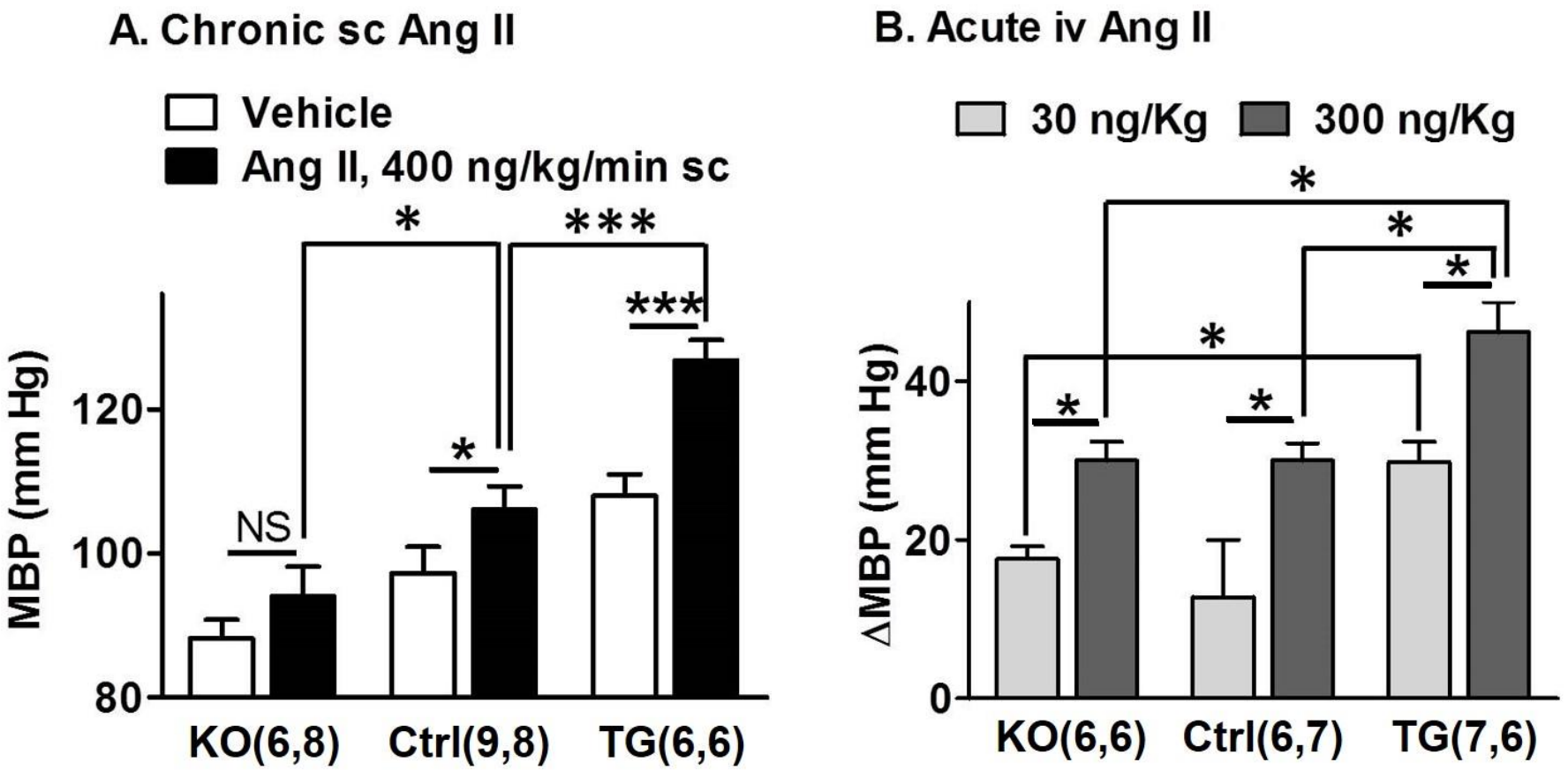

Fig. 6

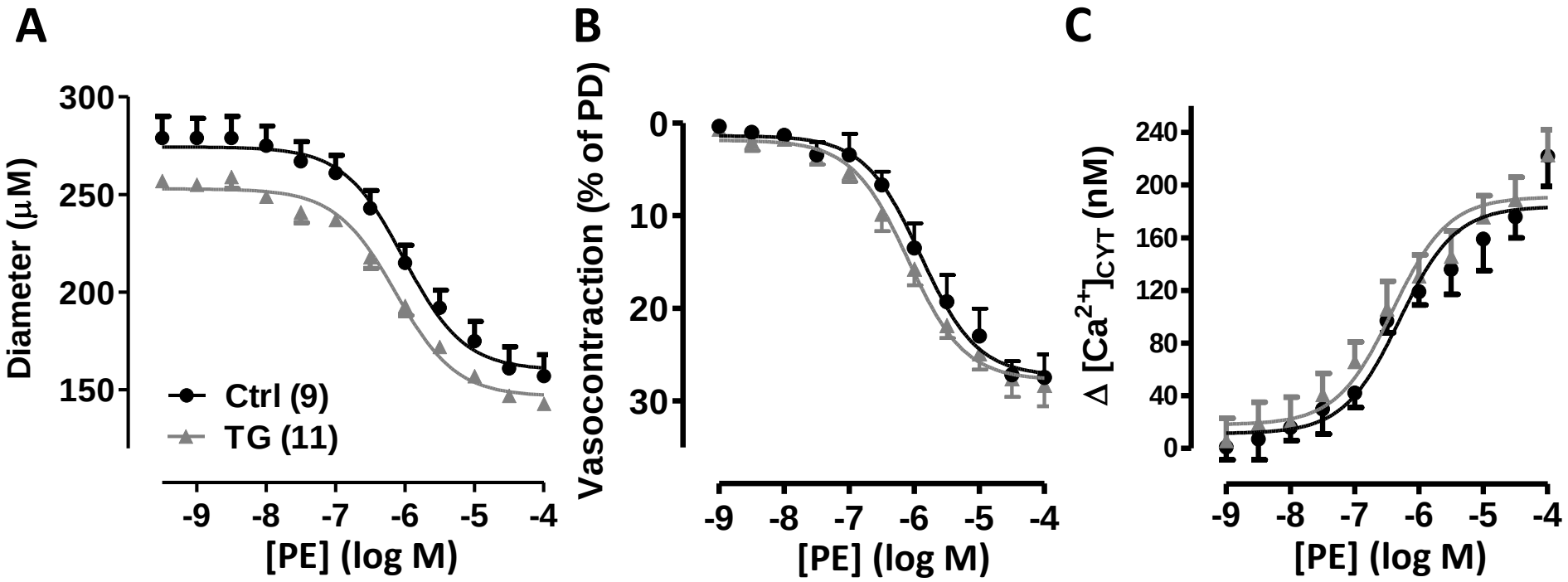

Fig. 7

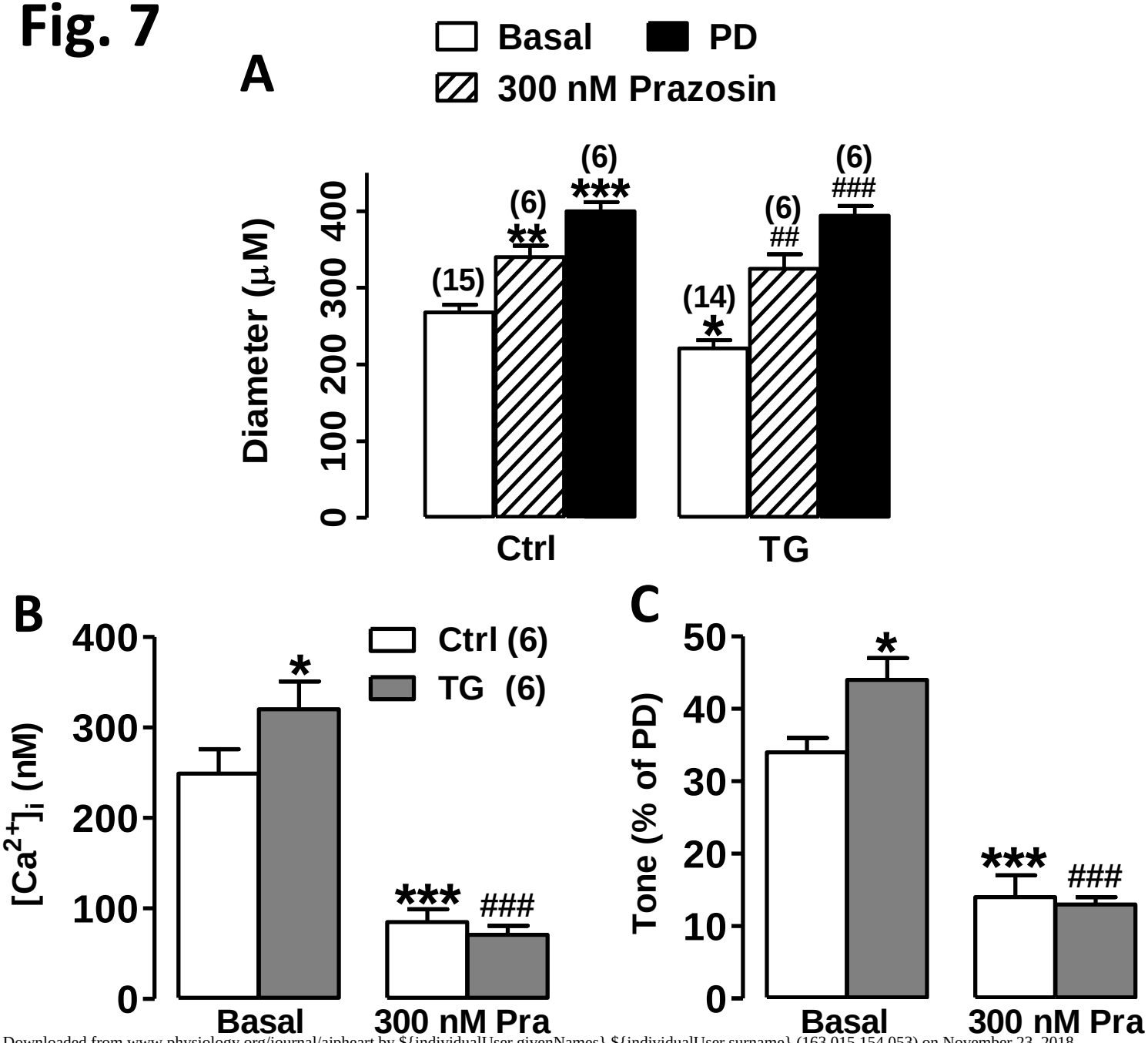

Fig. 8

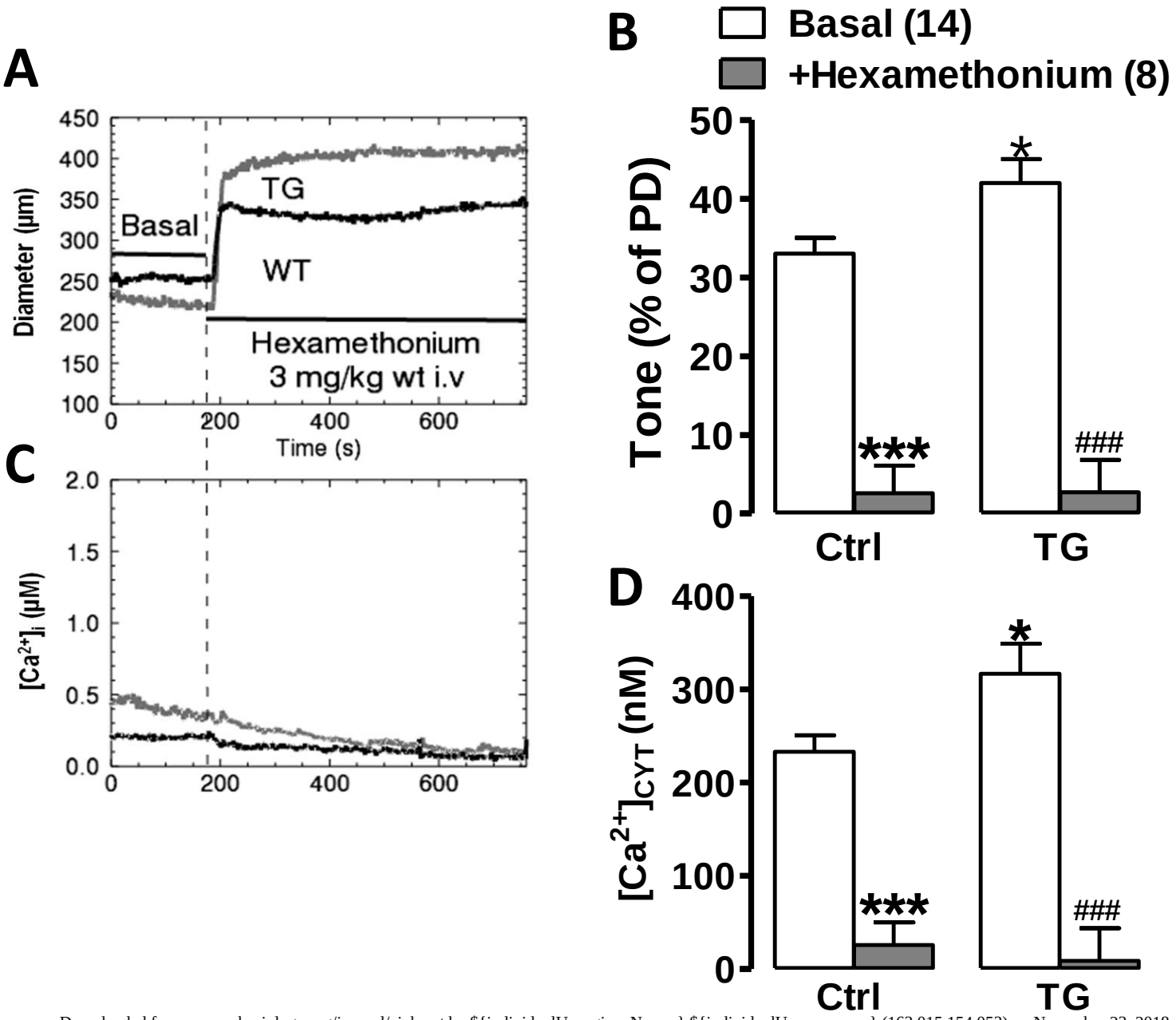

Fig. 9

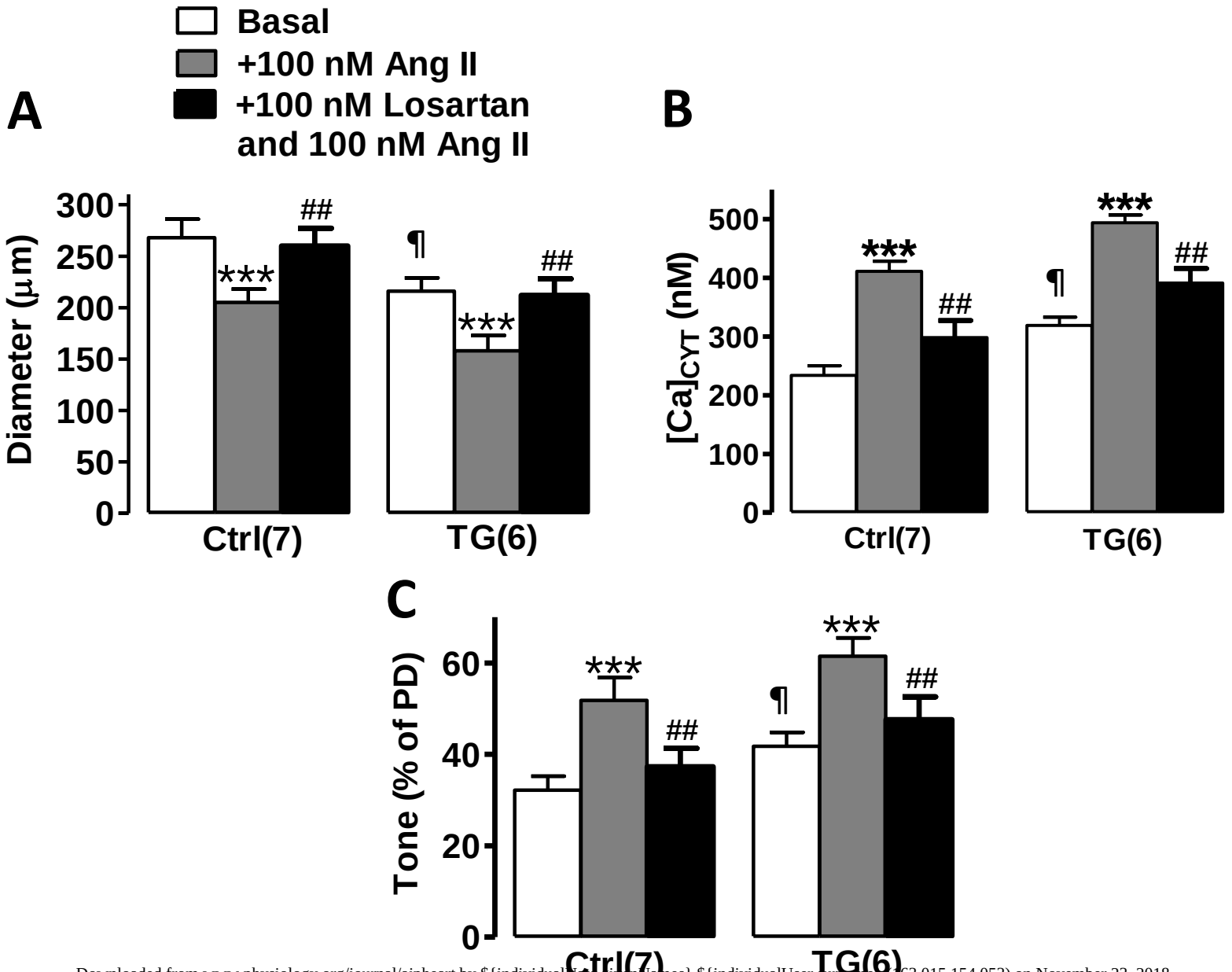

Fig. 10

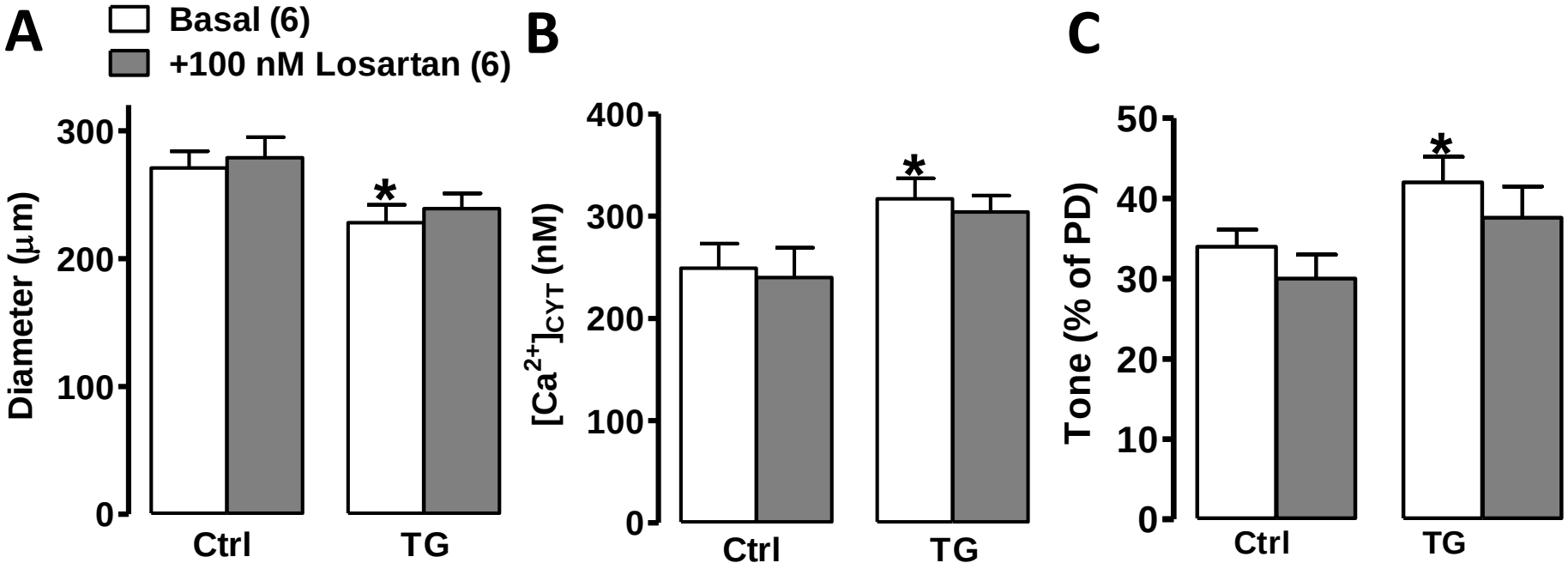

Fig. 11

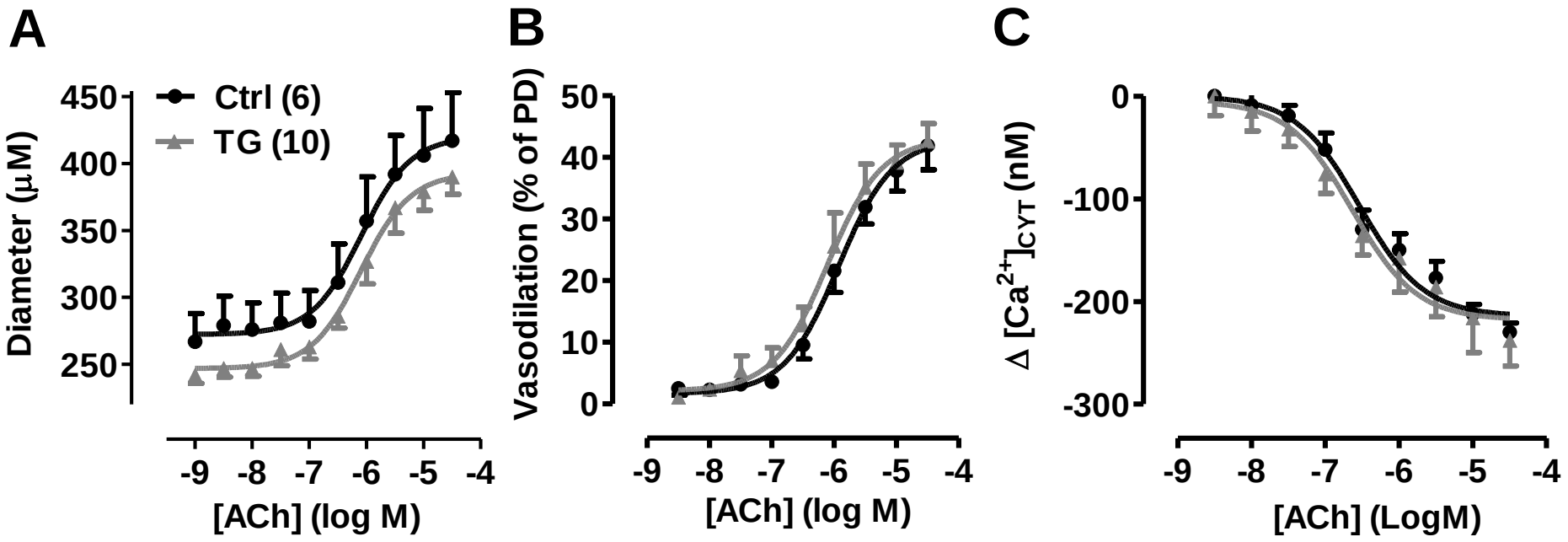

Fig. 12

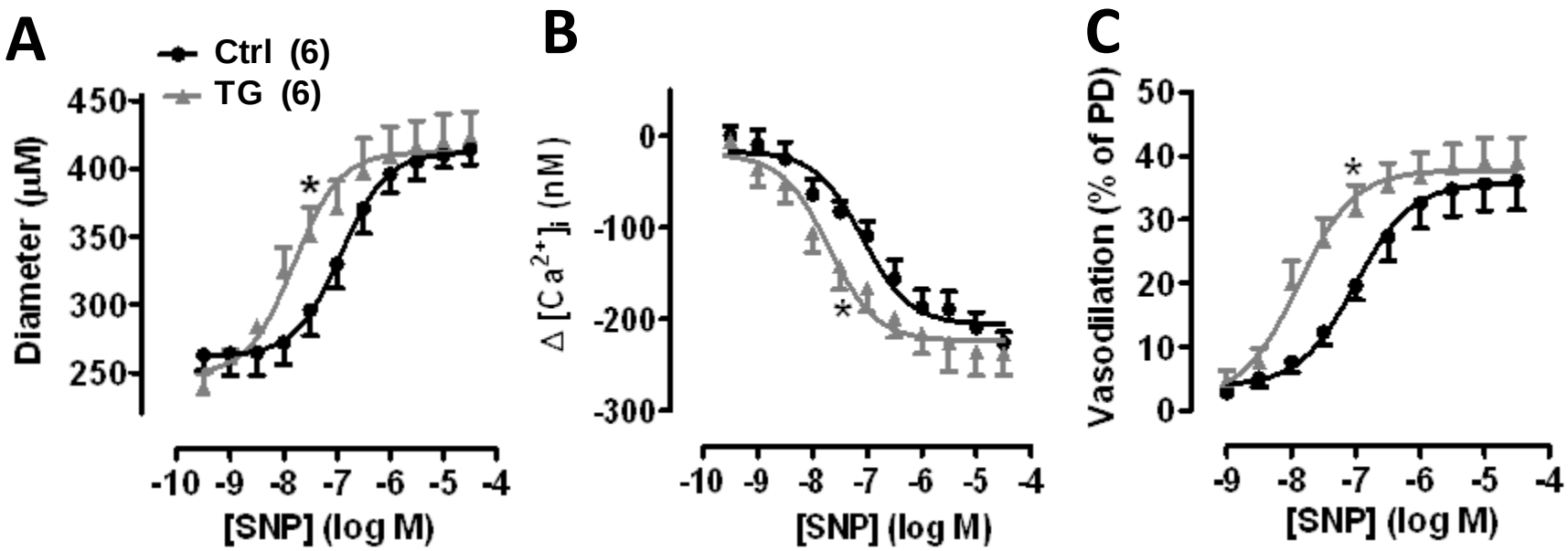

Fig. 13